© 2014. Published by The Company of Biologists Ltd | Development (2014) 141, 3431-3436 doi:10.1242/dev.115667

CORRECTION

Distinct roles of Polycomb group gene products in transcriptionally repressed and active domains of *Hoxb8*

Yu-ichi Fujimura, Kyo-ichi Isono, Miguel Vidal, Mitsuhiro Endoh, Hiroshi Kajita, Yoko Mizutani-Koseki, Yoshihiro Takihara, Maarten van Lohuizen, Arie Otte, Thomas Jenuwein, Jacqueline Deschamps and Haruhiko Koseki

There were errors published in *Development* **133**, 2371-2381.

The authors have become aware of errors with the display of data in Fig. 4E, Fig. 5A and Fig. 6. These errors are detailed below, and the authors have also provided the original data for these figures, which are included as part of the correction.

In Fig. 4E, the Rnf2 and trimH3-K27 lanes were spliced together without marking, removing intervening lanes from the original gel. In preparing the figure, the *Hoxb6* Rnf2 lanes were duplicated as *Hoxb8* Rnf2. In addition, contrast adjustments were applied to the original image that obscured weak bands in the *Rnf2*$^{-/-}$ lanes that we assume are the result of non-specific binding of chromatin to the beads during the immunoprecipitation procedure. Finally, the control lanes are wrongly labelled as *Hprt*; the negative control used for this experiment was in fact *Adam34*. These errors are corrected in the revised Fig. 4 and legend shown below, and the original data for this experiment are provided as 'Fig. 4E original data'.

Fig. 4 (revised)

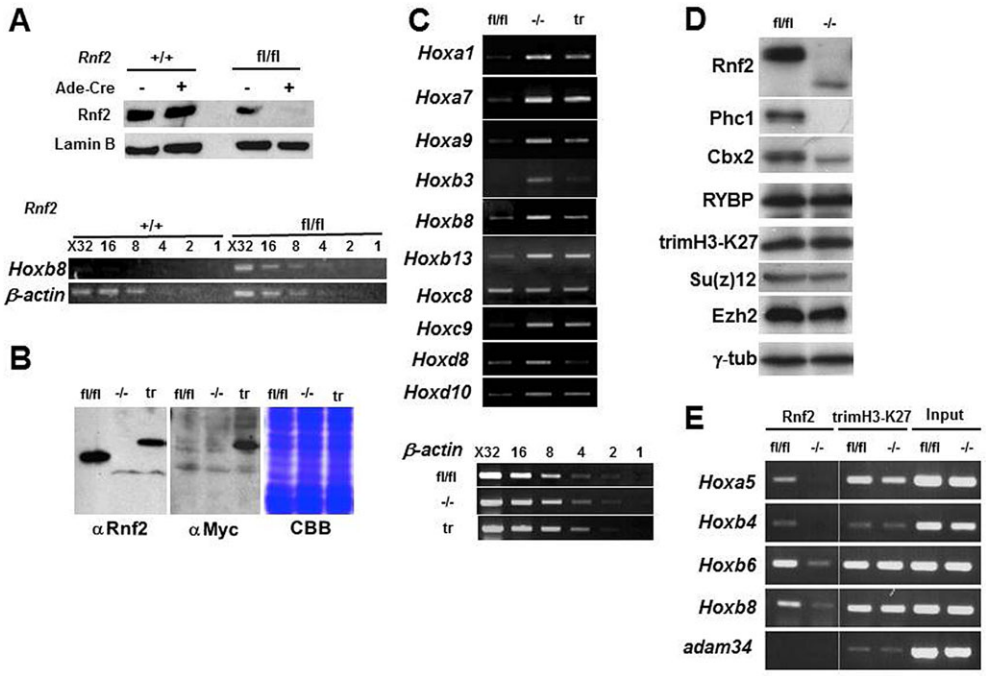

Fig. 4. De-repression of Hox genes in *Rnf2*$^{-/-}$ MEFs and ES cells. (**A**) Conditional depletion of Rnf2 leads to de-repression of *Hoxb8* in MEFs derived from the cranial part of *Rnf2*$^{fl/fl}$ 9.5 dpc embryos. (Top) Infection of Cre-expressing adenovirus vector to MEFs derived from *Rnf2*$^{fl/fl}$ embryos (fl/fl) depleted the Rnf2 gene products, whereas the wild-type (+/+) MEFs were unaffected. Lamin B was used as a control. (Bottom) The expression of Hoxb8 was induced by infection of Cre-expressing adenovirus vector in *Rnf2*$^{fl/fl}$ MEFs (fl/fl), but not in the wild type (+/+). (**B**) *Rnf2*$^{-/-}$ (–/–) ES cells were derived from *Rnf2*$^{fl/fl}$ (fl/fl) ES cells by transient overexpression of Cre-recombinase. Rnf2 was re-expressed by transfecting *Rnf2*$^{-/-}$ ES cells with a construct expressing Myc-tagged Rnf2 (tr). The expression of endogenous and transfected Rnf2 was examined by using anti-Rnf2 (left) and -Myc (middle) antibodies. CBB staining was used as a loading control (right). (**C**) The expression of Hox cluster genes in *Rnf2*$^{fl/fl}$ (fl/fl), *Rnf2*$^{-/-}$ (–/–) and Rnf2 transfected (tr) ES cells was compared by RT-PCR. The quantity of synthesized cDNA from respective cells was equalized by comparing the relative amounts of β-actin transcripts. (**D**) The expression of Phc1 and Cbx2 gene products was reduced in *Rnf2*$^{-/-}$ ES cells (–/–) in comparison with the wild type (fl/fl), whereas the expression of RYBP (another Rnf2-binding protein that is not found in hPRC-H complex or class 1 PcG proteins) was not altered. (**E**) Rnf2 association and H3-K27 trimethylation at Hox promoter regions were compared between *Rnf2*$^{fl/fl}$ and *Rnf2*$^{-/-}$ ES cells. For the 'Input', genomic DNA extracted from the original whole cell lysate equivalent to the 1/40 volume of that used for the ChIP analysis was subjected to the PCR. *Adam34* was used as a negative control. White lines indicate the removal of intervening gel lanes.

Development (2014) 141, 3431-3436 doi:10.1242/dev.115667

In Fig. 5A, for all samples except *Hoxa4*, the order in which the lanes are shown in the figure does not represent the order in which they were run on the original gel, where samples were run in the order: Suz12, Eed3, Rnf2, trimH3-K27, Input. For *Hoxb1* and *Hoxb4*, the lanes were exchanged in the figure but this splicing was not appropriately marked. For *Hoxb6* and *Hoxb8*, we failed to exchange these lanes and therefore the labelling was incorrect in the published figure. In addition, the control lanes were wrongly labelled as *Hprt*; the negative control used was *Adam34*. These errors are corrected in the revised Fig. 5 and legend shown below, and the original data for this experiment are provided as 'Fig. 5A original data'.

Fig. 5 (revised)

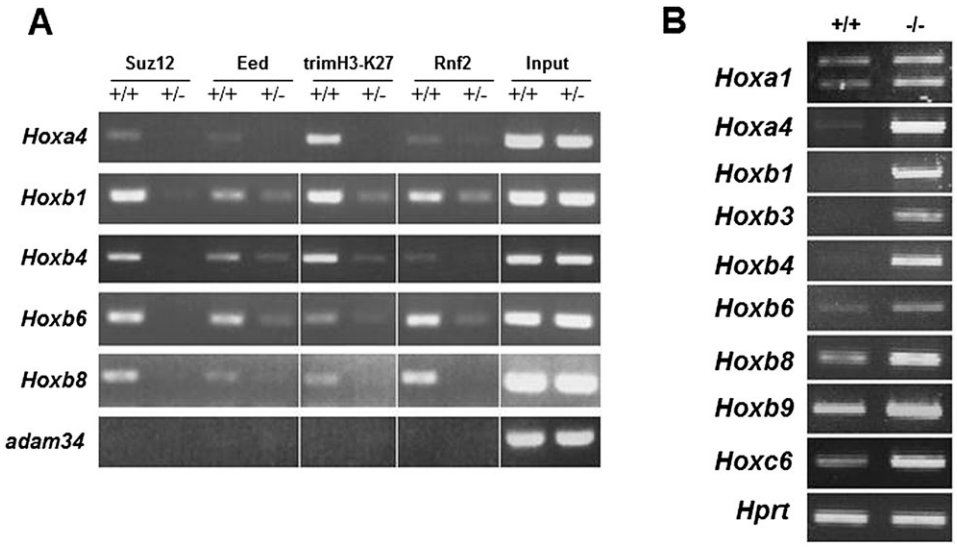

Fig. 5. De-repression of Hox genes in *Suz12*$^{-/-}$ ES cells correlates with reduction of Rnf2 association to Hox genomic regions. (**A**) The association of Suz12, Eed, Rnf2 and H3-K27 trimethylation at the Hox promoter regions in the wild-type and *Suz12*$^{-/-}$ ES cells. Whole-cell lysates prepared from approximately the same number of wild type (+/+) and *Suz12*$^{-/-}$ (–/–) ES cells were subjected to ChIP analyses using anti-Suz12, -Eed, -trimethylated H3-K27 and -Rnf2 antibodies. For the 'Input', genomic DNA extracted from the original whole cell lysate equivalent to the 1/40 volume of that used for the ChIP analysis was subjected to the PCR. *Adam34* was used as a control. (**B**) The expression of Hox cluster genes in the wild type (+/+) and *Suz12*$^{-/-}$ (–/–) ES cells was compared by RT-PCR. *Hprt* was used as a control. White lines indicate the removal of intervening gel lanes or their exchange.

In Fig. 6A, the original experiment included samples taken from *Rnf110*$^{+/-}$; *Bmi1*$^{-/-}$ animals. These were removed from the published version, but this splicing was not marked. In Fig. 6B, the original experiment included samples taken from *Phc1*$^{-/-}$; *Phc2*$^{+/-}$. We chose to show only data from the double heterozygote and double homozygote mutant, but in the case of *Hoxb8* accidentally removed the *Phc1*$^{+/-}$; *Phc2*$^{+/-}$ lanes instead of *Phc1*$^{-/-}$; *Phc2*$^{+/-}$. As can be seen in the original data, the results are highly similar for both genotypes. These errors are corrected in the revised Fig. 6 and legend shown below, and the original data for these experiments are provided as 'Fig. 6 original data'.

Fig. 6 (revised)

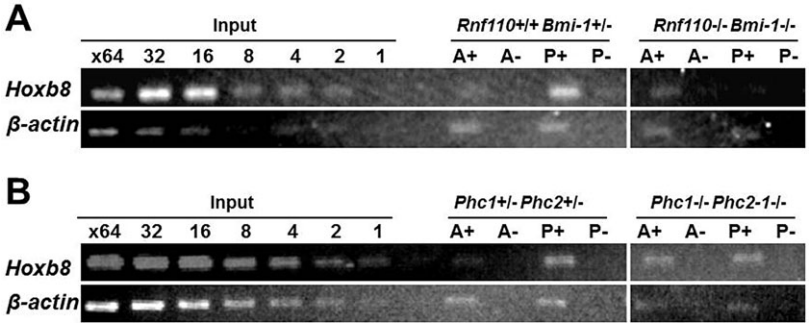

Fig. 6. Decreased H3-K9 acetylation at the first exonic region of *Hoxb8* in the posterior tissues of *Rnf110*$^{-/-}$*Bmi1*$^{-/-}$ and *Phc1*$^{-/-}$*Phc2*$^{-/-}$ embryos at 9.5 dpc. (**A**) Degree of H3-K9 acetylation in the anterior (A) and posterior (P) regions were compared in *Rnf110*$^{+/-}$*Bmi1*$^{+/-}$ and *Rnf110*$^{-/-}$*Bmi1*$^{-/-}$ embryos. The β-actin promoter was used as a positive control. (**B**) Degree of H3-K9 acetylation in the anterior (A) and posterior (P) regions were compared in *Phc1*$^{-/-}$*Phc2*$^{+/-}$, *Phc1*$^{+/-}$*Phc2*$^{-/-}$ and *Phc1*$^{-/-}$*Phc2*$^{-/-}$ embryos. The β-actin promoter was used as a positive control. In this study, the negative control ChIPs (A– and P–) were performed with rabbit IgG. White lines indicate the removal of intervening gel lanes.

Development (2014) 141, 3431-3436 doi:10.1242/dev.115667

The authors apologise to readers for these errors. The editors of the journal and the authors' Research Integrity Office have examined this paper in detail and find that, although there were substantive errors in data presentation, these do not affect the conclusions of the paper.

Fig. 4E original data

Without lane splicing:

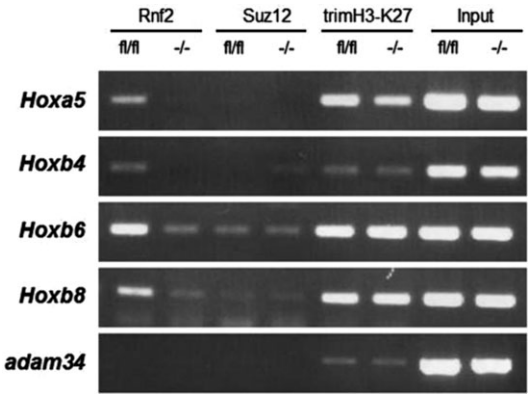

From laboratory notebook:

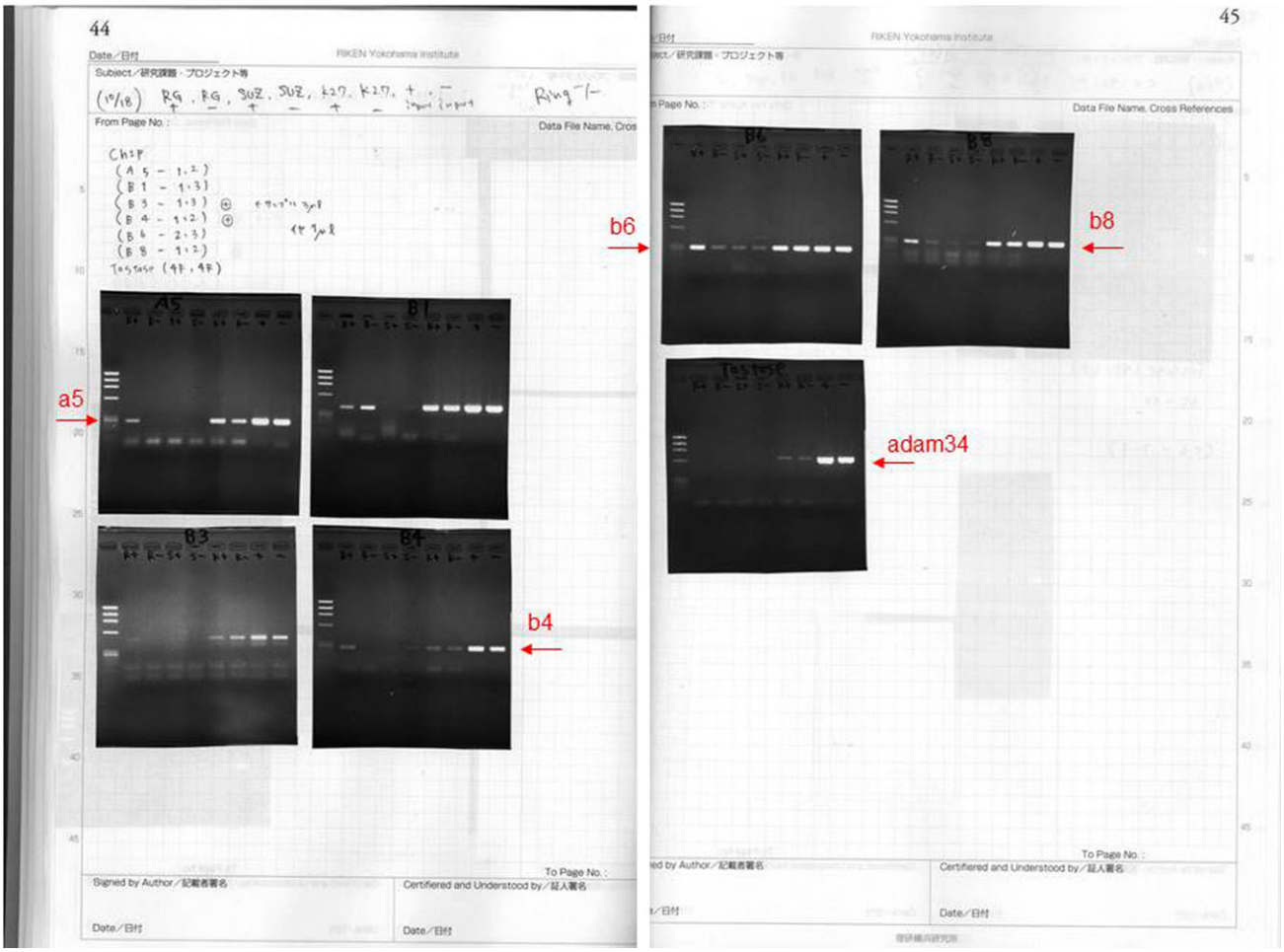

Development (2014) 141, 3431-3436 doi:10.1242/dev.115667

Fig. 5A original data

Without lane splicing:

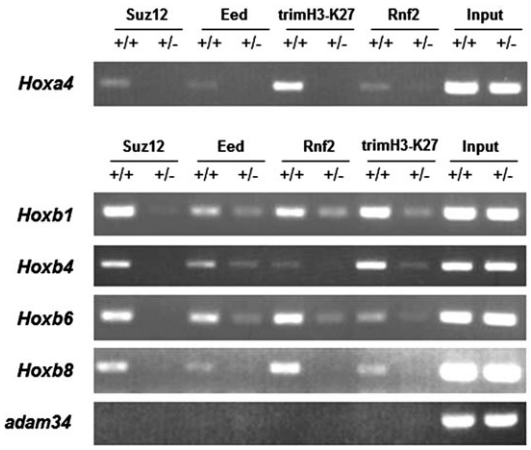

From laboratory notebook:

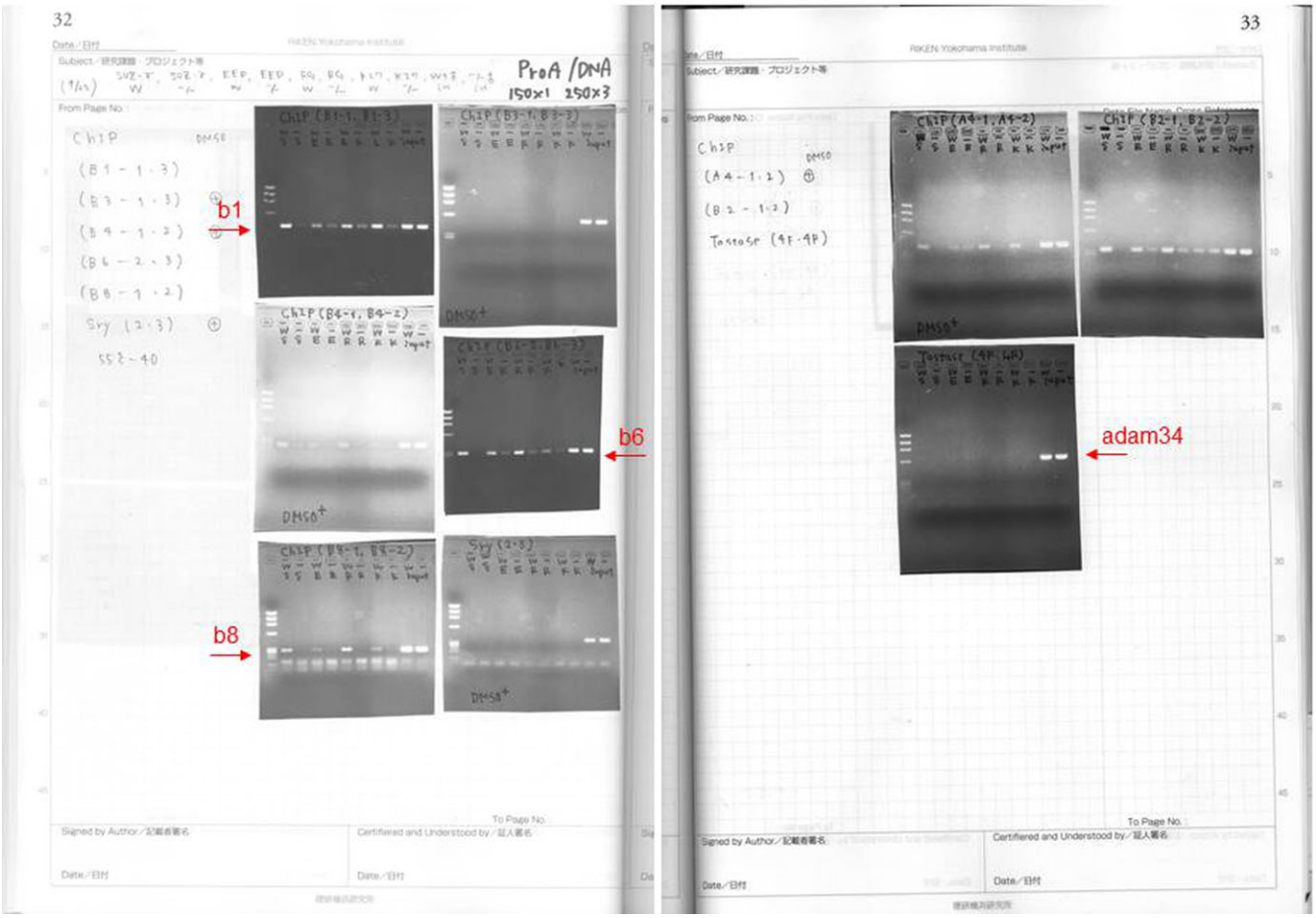

Development (2014) 141, 3431-3436 doi:10.1242/dev.115667

Fig. 5A original data (cont.)

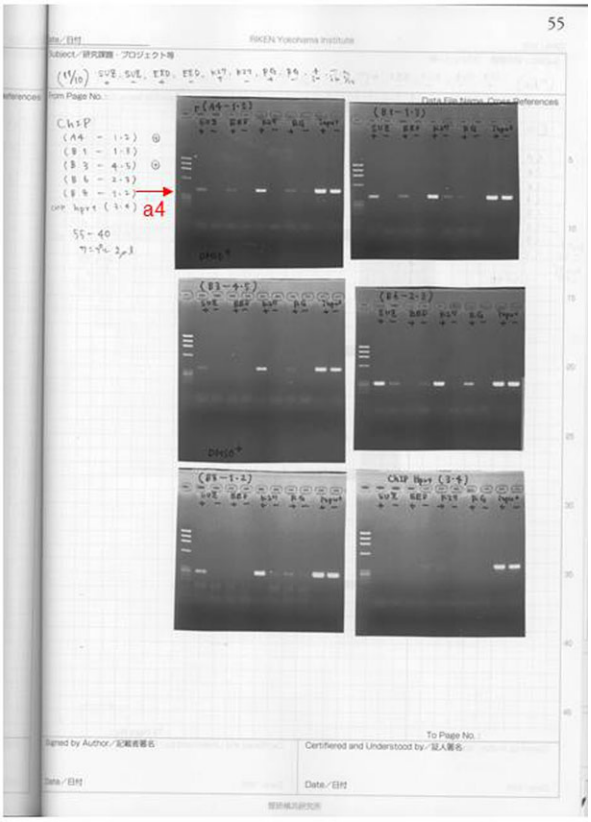

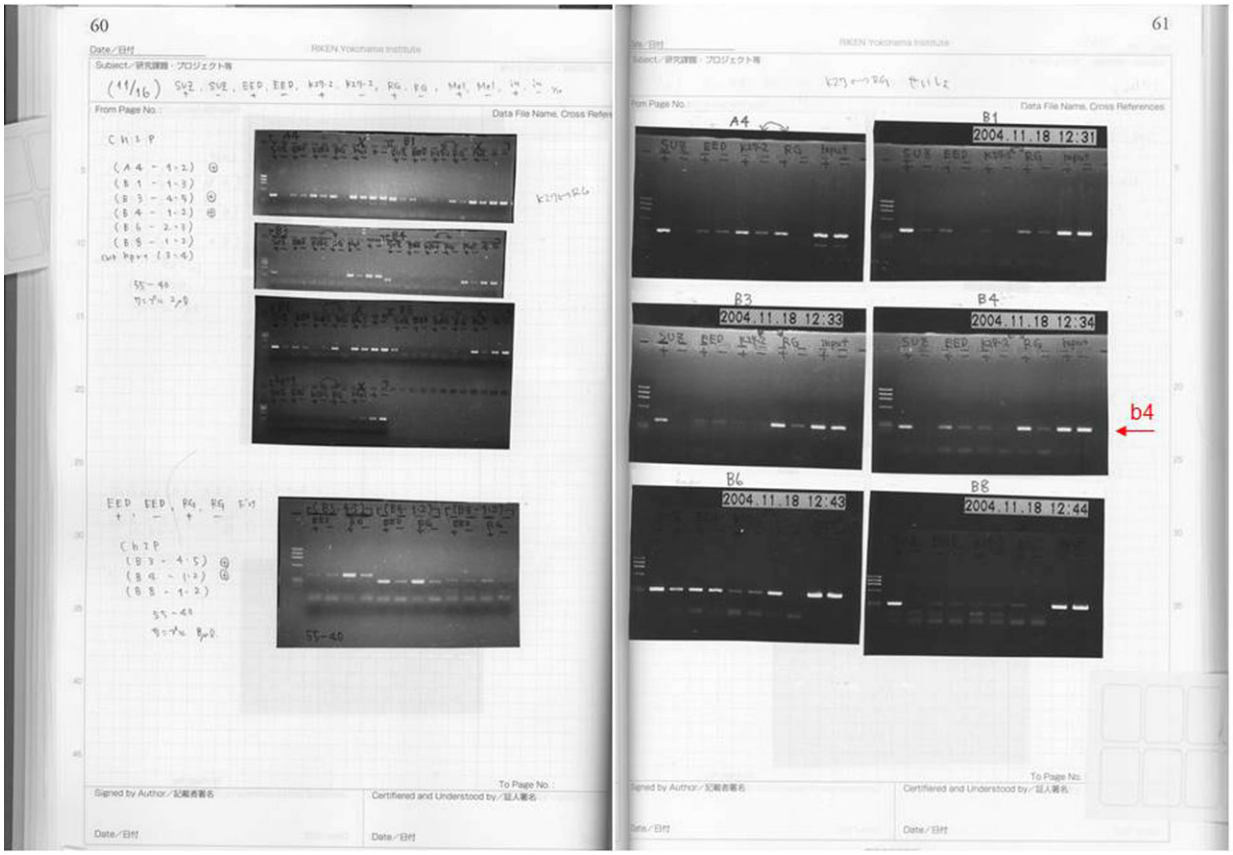

Development (2014) 141, 3431-3436 doi:10.1242/dev.115667

Fig. 6 original data

Without lane splicing:

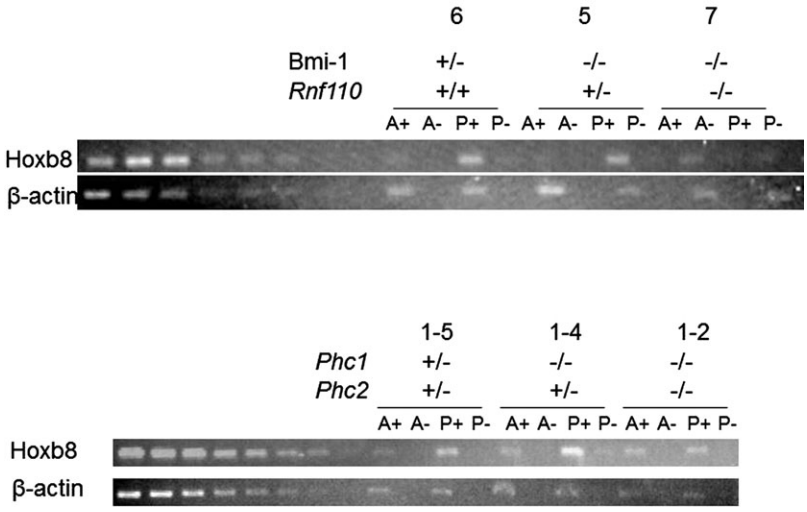

Development 133, 2371-2381 (2006) doi:10.1242/dev.02405

Distinct roles of Polycomb group gene products in transcriptionally repressed and active domains of *Hoxb8*

Yu-ichi Fujimura[1,*], Kyo-ichi Isono[1,*], Miguel Vidal[2], Mitsuhiro Endoh[1], Hiroshi Kajita[1], Yoko Mizutani-Koseki[1], Yoshihiro Takihara[3], Maarten van Lohuizen[4], Arie Otte[5], Thomas Jenuwein[6], Jacqueline Deschamps[7] and Haruhiko Koseki[1,†]

To address the molecular mechanisms underlying Polycomb group (PcG)-mediated repression of Hox gene expression, we have focused on the binding patterns of PcG gene products to the flanking regions of the *Hoxb8* gene in expressing and non-expressing tissues. In parallel, we followed the distribution of histone marks of transcriptionally active H3 acetylated on lysine 9 (H3-K9) and methylated on lysine 4 (H3-K4), and of transcriptionally inactive chromatin trimethylated on lysine 27 (H3-K27). Chromatin immunoprecipitation revealed that the association of PcG proteins, and H3-K9 acetylation and H3-K27 trimethylation around *Hoxb8* were distinct in tissues expressing and not expressing the gene. We show that developmental changes of these epigenetic marks temporally coincide with the misexpression of Hox genes in PcG mutants. Functional analyses, using mutant alleles impairing the PcG class 2 component Rnf2 or the *Suz12* mutation decreasing H3-K27 trimethylation, revealed that interactions between class 1 and class 2 PcG complexes, mediated by trimethylated H3-K27, play decisive roles in the maintenance of Hox gene repression outside their expression domain. Within the expression domains, class 2 PcG complexes appeared to maintain the transcriptionally active status via profound regulation of H3-K9 acetylation. The present study indicates distinct roles for class 2 PcG complexes in transcriptionally repressed and active domains of *Hoxb8* gene.

KEY WORDS: Polycomb, Hox, Mouse, Chromatin, Immunoprecipitation

INTRODUCTION

In *Drosophila*, the regionally restricted expression of homeotic genes (Hox genes) is maintained by two groups of proteins: the trithorax group (trxG) and Polycomb group (PcG). The trxG gene products are required to maintain the activity of Hox genes in the appropriate segments, whereas the PcG are involved in their repression (Paro, 1995; Pirrotta, 1997). Indeed, some of the PcG genes have been identified as suppressors of trxG mutations (Kennison and Tamkun, 1988). The *trxG* and *PcG* genes encode nuclear factors that, by forming multimeric protein complexes on the chromatin, freeze transcriptional states determined early in embryogenesis. A major function of trxG gene products appears to concern the remodeling of chromatin structure, as several of these genes encode subunits of the SWI/SNF chromatin remodeling complex and associate with catalytic activities that modify core histone tails (Milne et al., 2002; Nakamura et al., 2002; Tamkun et al., 1992). PcG gene products have been shown to form at least two types of multimeric protein complexes (Shao et al., 1999; Czermin et al., 2002; Muller et al., 2002; Cao et al., 2002). The first type of complex, known as class 1, includes Extra sex combs (Esc) and Enhancer of zeste [E(z)], and its association with histone deacetylase and methyltransferase activities suggests a function in the modification of histone tails (Czermin et al., 2002; Muller et al., 2002; Cao et al., 2002). The second type of complex (class 2) contains Polycomb (Pc), Posterior sex combs (Psc), Polyhomeotic (Ph), Dring (Sex comb extra; Sce) and Sex comb on midleg (Scm) in *Drosophila* (Shao et al., 1999). It has been shown that, by interacting with DNA regulatory sequences termed PcG response elements (PREs), this complex can maintain the transcriptional silence of target genes. Recently, it has been reported that class 1 PcG-mediated trimethylation of histone H3 lysine 27 (H3-K27) serves as a signal for the recruitment of class 2 PcG complexes, which in turn may silence target genes flanked by PREs (Cavalli and Paro, 1998; Wang et al., 2004b). Purified class 2 core complexes efficiently block SWI/SNF-dependent remodeling of nucleosomal arrays and subsequent transcription in vitro (King et al., 2002; Levine et al., 2002; Shao et al., 1999).

In mammals, it has been demonstrated that the expression of Hox cluster genes depends on the control of mammalian homologues of trxG and both classes of PcG gene products. Silencing of several Hox gene expressions has been observed in mice lacking *Mll*, a mammalian homologue of *Drosophila trx*, between 8.5 and 9.5 days post coitus (dpc) (Yu et al., 1998). Conversely, a hypomorphic mutation of *Eed*, a homologue of *Drosophila Esc*, revealed its involvement in repressing Hox gene expression (Schumacher et al., 1996). As Mll and class 1 PcG complex are known to be associated with activities that modify histone tails (van der Vlag and Otte, 1999), such modifications could be involved in maintaining spatially restricted expression of Hox cluster genes. Indeed, it has been shown that the Mll protein regulates the acetylation of lysine 4 of histone H3 (H3-K4) at several Hox genes, whereas Ezh2, a homologue of E(z), mediates H3-K27 trimethylation (Milne et al., 2002; Nakamura et al., 2002). The involvement of class 2 PcG in this maintenance has been revealed previously by the effect of mutations

[1]RIKEN Research Center for Allergy and Immunology, 1-7-22 Suehiro, Tsurumi-ku, Yokohama 230-0045, Japan. [2]Centro de Investigaciones Biologicas, Department of Developmental and Cell Biology, Ramiro de Maeztu 9, 28040 Madrid, Spain. [3]Department of Stem Cell Biology, Research Institute for Radiation Biology and Medicine, Hiroshima University, 1-2-3 Kasumi, Minami-ku, Hiroshima 734-8553, Japan. [4]Division of Molecular Genetics, The Netherlands Cancer Institute, 1066CX Amsterdam, The Netherlands. [5]Swammerdam Institute for Life Sciences, University of Amsterdam, Kruislaan 406, 1098 SM Amsterdam, The Netherlands. [6]Research Institute of Molecular Pathology, The Vienna Biocenter, Dr Bohrgasse 7, A-1030 Vienna, Austria. [7]Hubrecht Laboratory, Uppsalalaan 8 3584CT Utrecht, The Netherlands.

*These authors contributed equally to this work
[†]Author for correspondence (e-mail: fujimara@rcai.riken.jp)

Accepted 12 April 2006

in *Bmi1* (*Pcgf4* – Mouse Genome Informatics), *Rnf110* (*Mel18*; *Pcgf2* – Mouse Genome Informatics), *Phc1* (*rae28*) and *Rnf2* (*Ring1B*) on Hox gene expression (Akasaka et al., 1996; van der Lugt et al., 1996; Suzuki et al., 2002; Takihara et al., 1997). Notably, in mice doubly deficient for *Rnf110* and *Bmi1*, homologues of *Drosophila Psc*, *Hoxb6* expression was normally localized in caudal tissues of 8.5 dpc embryos, but was progressively de-repressed cranially thereafter (Akasaka et al., 2001). Thus, class 2 PcG proteins may participate in maintaining transcriptionally silent states of Hox genes outside their expression domains. However, to date, the molecular mechanisms used by mammalian trxG and PcG gene products to regulate Hox genes is not well understood, in part because the relationship between PcG protein binding and histone tail modifications has not yet been widely documented around the Hox loci in developing embryos. We have addressed this issue by documenting the association of PcG proteins, H3-K9 acetylation, H3-K4 methylation (marks of transcriptionally active chromatin) and H3-K27 trimethylation (a mark of transcriptionally inactive chromatin) to the genomic region flanking *Hoxb8*, a Hox gene known to require the class 2 PcG proteins for its posterior restriction.

We show that the association of PcG proteins, H3-K9 acetylation, H3-K4 methylation and H3-K27 trimethylation around *Hoxb8* differs in embryonic tissues expressing and not expressing the gene. By using mutant alleles for *Rnf2*, which encode constituents of class 2 PcG complexes, and *Suz12* causing a strong decrease in H3-K27 methylation, we show that the recruitment of the class 2 PcG complex, mediated by trimethylated H3-K27, plays a decisive role in maintaining the repression of Hox genes outside their expression domain, as it is the case in *Drosophila*. The positive role of class 2 PcG complex proteins in the transcriptionally active domain was shown to involve the regulation of H3-K9 acetylation.

MATERIALS AND METHODS

Mice and cell lines

The generation of $Rnf2^{fl}$ allele and Rnf2 mutant ES cells has been described previously (de Napoles et al., 2004). The generation of *Suz12*-deficient mice and ES cells will be described in a separate publication. CRE-mediated deletion of Rnf2 in MEF cell lines using adenovirus expressing the CRE recombinase (AdCre) was carried out as described (Kanegae et al., 1995). AdCre virus was concentrated to be 2.0×10^{-9} i.f.u./ml and mouse embryonic fibroblast (MEFs) were infected with AdCre virus at MOI5.

Antibodies

Antibodies used are listed in the Table 1.

Chromatin immunoprecipitation (ChIP) analysis

Embryonic tissues of interest were dissected from embryos, at the different developmental stages, under a stereomicroscope. Chromatin fraction from the embryonic tissues was purified by CsCl isopycnic centrifugation as described in Fig. S1 in the supplementary material (Orlando et al., 1997). This process was bypassed in some cases. Correct amounts of NaCl and NP-40 were added to the chromatin fraction or whole cell lysates (WCE) in order to perform optimal immunoprecipitation for each antibody. Precleared protein extracts were incubated with the correct amount of antibodies, at 4°C with rocking, for 2 hours to overnight. Immune complexes were captured after 3 hours incubation with Protein A Sepharose beads.

To isolate genomic DNA from immune complexes, beads were treated with 50 μg/ml of RNaseA at 37°C for 30 minutes followed by overnight incubation with 500 μg/ml proteinase K/0.5% SDS at 37°C. After 3 hours heating at 65°C for reverse crosslinking, supernatants were collected, extracted by phenol-chloroform and concentrated by ethanol precipitation. Genomic DNA was also isolated from the original chromatin fraction or WCE through the same procedure as described above and designated as 'Input' DNA (see Figs 1-3). To measure the DNA yield after immunoprecipitation, the aliquots of immunoprecipitated DNA were electrophoresed for 5 minutes in an agarose gel, next to serially diluted input DNA and band-intensities were compared after ethidium bromide staining (see Fig. S2A in the supplementary material).

Equivalent amounts of immunoprecipitated DNA to that of 'Input' DNA loaded in lane '1' were subjected to PCR reactions. Usually, 10 to 20 ng of genomic DNA was used. Mock-immunoprecipitated DNA (A– and P–) derived from the same volume of the chromatin fraction as used for anti-Rnf2 immunoprecipitation were subjected to the PCR. To carry out semi-quantitative PCR, serially diluted 'Input' DNA and immunoprecipitated DNA were used as templates. The relative quantity of each genomic region in immunoprecipitated genomic DNA was estimated by referring to the serial dilutions of 'Input' DNA isolated from the initial lysates and an enrichment value was determined. Every series of experiments were performed at least three times (see Fig. S3 in the supplementary material). Primers used in this study are listed in Table 2. ChIP analysis by using ES cells was performed as described (Isono et al., 2005a).

Expression analyses for RNA and protein

RNA extraction from ES cells, reverse transcription and PCR reaction was performed as described previously (Isono et al., 2005a). Quantity of total cellular RNA subjected to reverse transcriptase (RT)-PCR for Hox genes was adjusted by the expression of β-actin. *Hoxb8* expression shown in Fig. 3A was quantified by referring to *Gapdh* expression by real-time PCR analyses using Mx3005P multiplex quantitative PCR systems (Stratagene). Preparation of whole-cell extracts from embryos, ES cells and MEFs and western blot analysis were performed as described previously (Isono et al., 2005a).

Table 1. A list of antibodies used in this study

Specificity	Species	Monoclonal or antiserum?	Company or reference
Rnf2	Mouse	Monoclonal	Atsuta et al. (2001)
Ring1	Rabbit	Antiserum	Schoorlemmer et al. (1997)
Phc1	Mouse	Monoclonal	Miyagishima et al. (2003)
Phc1	Rabbit	Antiserum	Suzuki et al. (2002)
Cbx2	Rabbit	Antiserum	Schoorlemmer et al. (1997)
Rnf110	Rabbit	Antiserum	Abcam (Cambridge, UK)
Eed	Mouse	Monoclonal	Hamer et al. (2002)
Ezh2	Mouse	Monoclonal	Hamer et al. (2002)
Suz12	Rabbit	Antiserum	Upstate Biotechnology (Lake Placid, NY)
Acetylated H3-K9	Rabbit	Antiserum	Upstate Biotechnology (Lake Placid, NY)
Dimethylated H3-K9	Rabbit	Antiserum	Peters et al. (2003)
Trimethylated H3-K9	Rabbit	Antiserum	Peters et al. (2003)
Dimethylated H3-K27	Rabbit	Antiserum	Peters et al. (2003)
Trimethylated H3-K27	Rabbit	Antiserum	Peters et al. (2003)
Dimethylated H3-K4	Rabbit	Antiserum	Upstate Biotechnology (Lake Placid, NY)
Trimethylated H3-K4	Rabbit	Antiserum	Upstate Biotechnology (Lake Placid, NY)

Table 2. PCR primers used in this study

Primer		Forward	Reverse	Positions*
Hoxb8 proximal	1	aacaggagacagagaaactggtac	actgtttgctttgctgctgtttag	1-516
	2	gggtataaatttctgaaggttaag	agggatgagaagggccgaggg	446-1006
	3	tatgactacctcgttgtttg	caaagactgatgtgggggagt	4292-4565
	4	ggtgtttttccgtgactcccccac	tagaacagcgaagcctgcaaaagt	4531-5091
	5	gccgcggctgccatgcaggcttag	cacggcgcacgggttctgctggta	5045-5568
	6	ttctacggctacgaccctctgcag	cttgagggcgcatccaggg	5593-5764
	7	ccctggatgcgccctcaag	tctccacagcccccataaaac	5746-6083
	8	actgttttatgggggctgtggaga	tctctggtaactagaaccag	6060-6315
	9	tggagctggagaaggagttccta	cagaagctattacgagatactacc	6592-7041
	10	ctccttcccttctcttgggggtcc	caatgctcacagcgcgcatgc	7061-7529
	11	ttagcatgcgcgctgtgagcattg	cactagccaccagcctgggta	7560-8032
	12	cgctcttgggaagagatctaccca	cccaagaggaggcgagcctgg	7994-8584
	13	aggccaggctcgcctcctcttggg	agtcggggacgttttagtgtc	8561-9085
	14	tcacgtggtcagaagagg	ctgagcttcgcatccaggggta	8978-9505
	15	tacccctggatgcgaagctcag	ctagggcctgagagcactgagc	9484-9706
	16	gctcagtgctctcaggccctag	acacccagaactgagctctc	9685-9927
	17	gagagctcagttctgggtgt	accactctttgactctgtgt	9908-10134
	18	acacagagtcaaagagtggt	gtcatctttctggagtgata	10115-10323
	19	tatcactccagaaagatgac	atgagtataggagtctct	10304-10527
	20	agagactcctatactcat	tctgagaactcccagcata	10501-10792
	21	tatgctgggagttctcaga	ctgacagaacttggctctgatg	10774-10985
	22	catcagagccaagttctgtcag	ctgtcatcagtcactctct	10964-11218
	23	agagagtgactgatgacag	agccatcctcctgattcag	11220-11408
	24	ctgcacctagtagtg	tgtaggtctggcggcctcgcttt	11581-11787
	25	ttgtaagccctctttgaagct	taacataaccctcctggcaggccg	12309-12829
Hoxb8 distal	D1	ggtagtagctttctgatggt	aggatgcaaactccattata	
	D2	accatcagaaagctactacc	aacgaatttattgagaattc	
Hoxb3		atgcagaaagccacctacta	ttggacgtttgcctcgactc	
Hoxb6		atgagttcctatttcgtgaa	accagccggcggcggctacg	
Hoxb8		atgagctcttatttcgtcaa	gcttgcagtctgcgtactgc	
Hoxb9		atgtccatttctgggacgct	tggtagacagacggcaggct	
Hoxa4		agctccagccctggcttcgc	cgtgatggatgcygctagcc	
Adam34		atgagtgggactaaggccctg	gcggttatgatctattactac	

*Position of 5′-most nucleotide of region 1 was arbitrarily designated as ‘1’.

RESULTS

Association of mammalian PcG proteins to the *Hoxb8* genomic region at 12.5 dpc

First, the issue of whether PcG-silencing of Hox genes in developing embryos involves the direct binding of PcG gene products to Hox genes was addressed. PcG associations at genomic regions flanking *Hoxb8* were compared between transcriptionally repressed cranial and active caudal tissues by ChIP using embryonic tissues at 12.5 dpc. As the rostral boundary of *Hoxb8* expression is at the level of the 7th prevertebrae in the paraxial mesoderm and at the caudal hindbrain in the neural tube, embryos were dissected transversely at the levels of the pinna primordium and posterior edges of the forelimb buds, after the removal of internal viscera and hindlimb buds. Only cranial and caudal tissues were subjected to the analysis (Fig. 1A). Chromatin fractions of the respective embryonic tissues were purified and subjected to immunoprecipitation using antibodies against Rnf2, Phc1, Ring1, Cbx2 and Rnf110 (see Fig. S1 in the supplementary material) (Suzuki et al., 2002). Quantity of immunoprecipitated genomic DNA was measured by referring to serially diluted genomic DNA isolated from the initial lysates (see Fig. S2A in the supplementary material). Usually, for a given volume of chromatin fraction, the amount of DNA immunoprecipitated by anti-Rnf2 antibodies was four- to eightfold higher than that brought down in the absence of primary antibody (see Fig. S2A in the supplementary material). Amounts of DNA from respective tissues were further adjusted by PCR for the *tbx2* gene, which is also bound by Rnf2 in embryonic tissues (see Fig. S2B in the supplementary material). Equivalent amounts of DNA immunoprecipitated from the anterior and posterior tissues were subjected to semi-quantitative PCR using pairs of primers defining discrete regions in the *Hoxb* locus (Fig. 1F, top; see Table 2). Serially diluted genomic DNA isolated from the initial lysates was also subjected to the PCR to evaluate the enrichment value for each region of *Hoxb8* in immunoprecipitated materials (Fig. 1B-E). The *adam34* gene, which is expressed exclusively in adult testes, is not bound by any of Rnf2, Ring1, Phc1, Cbx2 or Rnf110 in embryonic tissues and thus turned out to serve as a negative control (Brachvogel et al., 2002) (Fig. 1B-E).

The association of Rnf2 with regions 1, 2, 3, 9, 10, 11, 13, 15, 16 and D1 was more than four times different in cranial and caudal tissues, whereas this was not the case for regions 4, 5, 6, 7, 8, 12, 14, 19, 20, 21, 22, 23, 24, 25 or D2 (Fig. 1B,F, Supplemental Fig. 3). In region 17 and 18, no significant association of Rnf2 was observed. Regions 1 and 2, and 10 and 11, correspond to the *Hoxb8* regulatory regions BH1100 and KA that have previously been identified by transgenic approaches; regions 3 and 13 include the promoters of *Hoxb8* and *Hoxb7*, respectively (Charité et al., 1995; Vogels et al., 1993). Therefore, Rnf2 differentially binds to the proximal cis-regulatory elements of 5′ *Hoxb* genes in cranial and caudal embryonic tissues. Likewise, a significant differential association of Rnf2 to the distal element (DE) located between *Hoxb4* and *Hoxb5*

(Oosterveen et al., 2003) was also seen in cranial and caudal tissues. Similar to Rnf2, Ring1 association was seen in cranial tissues, except for regions 3 and 7 (Fig. 1D). In contrast to Rnf2 binding, the association of Phc1 extended through all regions examined except for region 8, without any obvious differences between cranial and caudal tissues (Fig. 1C). Nevertheless, in region 3, the association did appear to be significantly stronger in the caudal tissues. Furthermore, there was no significant difference between cranial and caudal tissues with respect to the chromatin association of Cbx2 (Fig. 1D). Therefore, these results indicate that Phc1 and Cbx2 are bound to *Hoxb8* genomic region irrespective of the transcriptional state of the gene. Rnf110 association to regions 3 and 10 was seen in the cranial tissues only, but to regions 1, 2, 7 and 14 it was seen in both cranial and caudal tissues (Fig. 1E). These experiments were

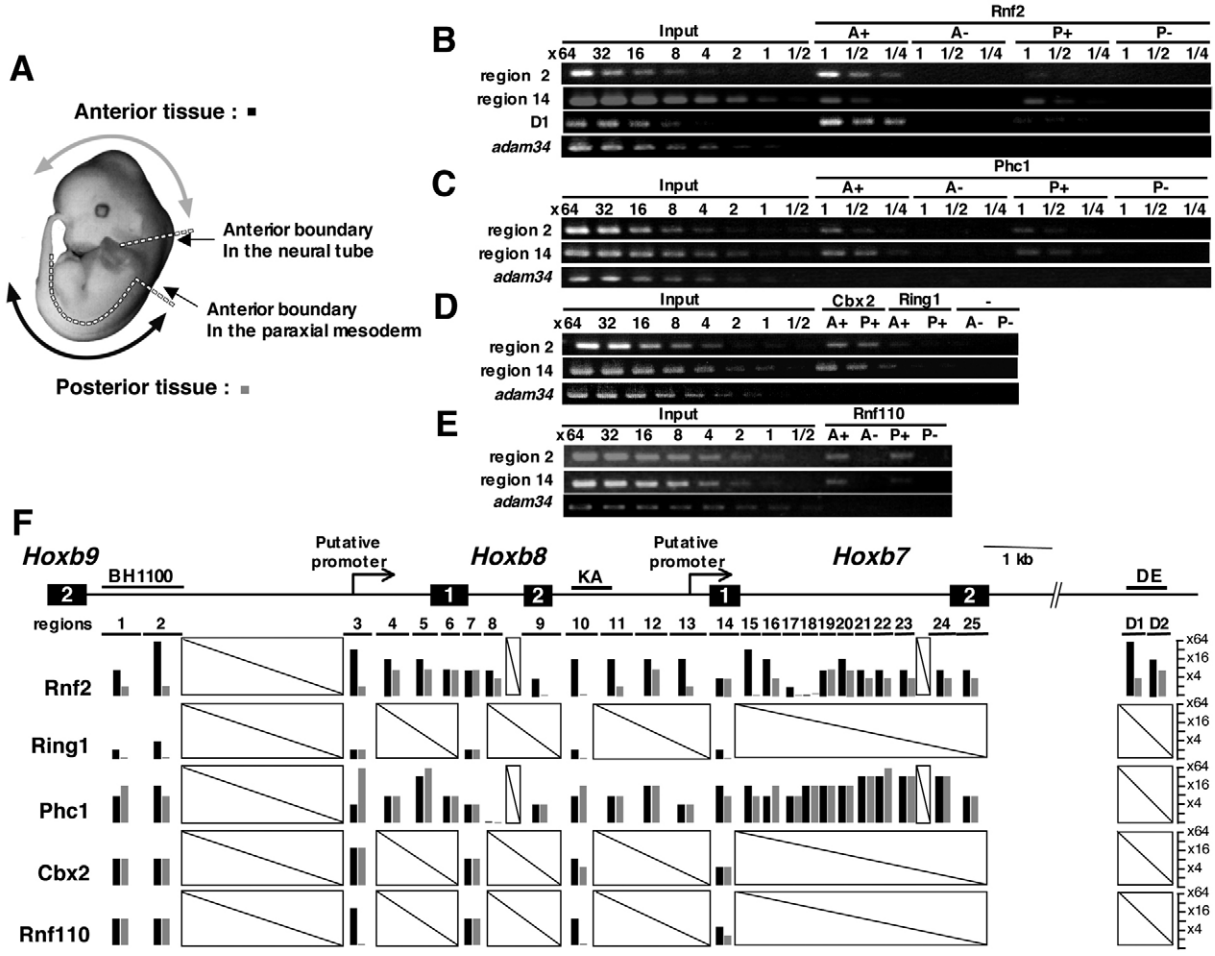

Fig. 1. Comparison of PcG associations with *Hoxb8* genomic surrounding at 12.5 dpc between anterior and posterior tissues. (**A**) Embryonic tissues used in this study. Wild-type embryos at 12.5 dpc were dissected as illustrated and anterior (A) and posterior (P) tissues (paraxial mesoderm plus neuroectoderm) were subjected to the ChIP analyses. (**B**) Comparative analysis of Rnf2 association to regions 2, 14 and D1 between anterior and posterior tissues. The chromatin fraction purified from A or P tissue was subjected to the immunoprecipitation with anti-Rnf2 antibody. Amounts of genomic DNA immunoprecipitated by anti-Rnf2 (A+ or P+) were quantified by comparing with serially diluted genomic DNA isolated from the original chromatin fractions designated as 'Input' (see Fig. S2A in the supplementary material) and equivalent amounts of immunoprecipitated DNA to that of 'Input' DNA loaded into lane 1 were subjected to PCR reactions. Usually 10 to 20 ng of genomic DNA was used. Immunoprecipitated DNA was also serially diluted. Mock-immunoprecipitated DNA (A– and P–) derived from the same volume of the chromatin fraction as used for anti-Rnf2 immunoprecipitation were subjected to the PCR. The *adam34* locus was used as a negative control. (**C**) Comparative analysis of Phc1 association to regions 2 and 14 between anterior and posterior tissues. (**D**) Comparative analyses for association of Cbx2 and Ring1 to regions 2 and 14. Amounts of genomic DNA (A+ and P+) immunoprecipitated by anti-Cbx2 and anti-Ring1 antibodies subjected to PCR were equivalent to that of 'Input' DNA loaded into lane 1. Mock-immunoprecipitated DNA (A– and P–) derived from the same volume of the chromatin fraction as used for anti-Cbx2 and -Ring1 immunoprecipitation were subjected to the PCR. (**E**) Rnf110 association to regions 2 and 14. All experiments were conducted as described using anti-Rnf110 antibody. (**F**) Schematic comparisons of Rnf2, Ring1, Phc1, Cbx2 and Rnf110 association to the *Hoxb8* genomic surrounding between anterior and posterior tissues. Genomic organization around *Hoxb8* gene is shown at the top. Exonic regions are indicated by black boxes and the exon numbers are numerically shown in the boxes. Positions of known cis-acting regulatory elements are represented by overlying bold bars indicated as BH1100, KA and DE (Charité et al., 1995; Vogels et al., 1993; Oosterveen et al., 2003). Putative promotor regions are indicated by folded arrows. The genomic regions examined by PCR using specific primer pairs listed in Table 1 are shown by bars and numerically indicated. The relative quantity of each genomic region in immunoprecipitated genomic DNA from anterior and posterior tissues was estimated by referring to 'Input' DNA isolated from the initial lysates and enrichment values against the 'Input', and are represented by the black and gray bars, respectively. Genomic regions left unexamined are covered by boxes crossed with a diagonal line.

performed three times with similar results (see Fig. S3 in the supplementary material). In summary, the complete form of the class 2 PcG complexes predominantly associate with *Hoxb8* in tissues where the gene is repressed, whereas form(s) lacking at least the Rnf2 component also bind in tissues actively expressing the Hox gene.

Differences between H3-K9 acetylation and H3-K27 trimethylation at *Hoxb8* in cranial and caudal embryonic tissues

Following this, the issue of the degree of H3-K9 acetylation and H3-K4 methylation at *Hoxb8* genomic regions in expressing and non-expressing embryonic tissues, was addressed. These epigenetic marks have been shown to be one of the prerequisites for the efficient recruitment of TBP through the interaction of TAF1 with the H3-K9 and K14 acetylated residues (Agalioti et al., 2002). A linear correlation between histone modifications and the transcriptional state of Hox genes has been seen in developing embryos at *Hoxd4* locus and MEFs that are derived from *Mll* mutants and wild-type controls (Rastegar et al., 2004; Milne et al., 2002). Therefore, as H3-K9 acetylation and H3-K4 methylation may be prerequisites for active transcription of Hox genes, these extents were compared between anterior and posterior embryonic tissues. H3-K9 acetylation and H3-K4 methylation around the *Hoxb8* was more abundant in the transcriptionally active caudal embryonic part than in the non-expressing anterior part as reported by Rastegar et al. (Rastegar et al., 2004) (Fig. 2A,B).

The methylation of H3-K9 and H3-K27 constitutes imprints for transcriptionally silent chromatin and is involved in many functions, including the formation of centromeric heterochromatin, X inactivation, PcG-mediated gene silencing and transcriptional repression at euchromatic positions (Fischle et al., 2003; Lachner et al., 2003). In particular, trimethylation of H3-K27 has been shown to be mediated by class 1 PcG complexes (Cao et al., 2002). The degree of H3-K9 and H3-K27 methylation at regions 2, 3 and 8 was compared between cranial and caudal embryonic regions. At all the regions examined, H3-K27 trimethylation was more abundant in the transcriptionally silent cranial embryonic part than in the Hox-expressing caudal part (Fig. 2B). No significant levels of di- or trimethylation of H3-K9 or dimethylation of H3-K27 were seen at any of the regions examined (Y.F. and H.K., unpublished).

Developmental kinetics of Rnf2-association and of histone H3 modifications at *Hoxb8*

Loss of spatial restriction of *Hoxb6* expression, between 8.5 and 9.5 dpc, has been reported as resulting from the *Rnf110/Bmi1* double mutation (Akasaka et al., 2001). Similarly, *Mll* deficiency progressively silences Hox gene expression within this time window

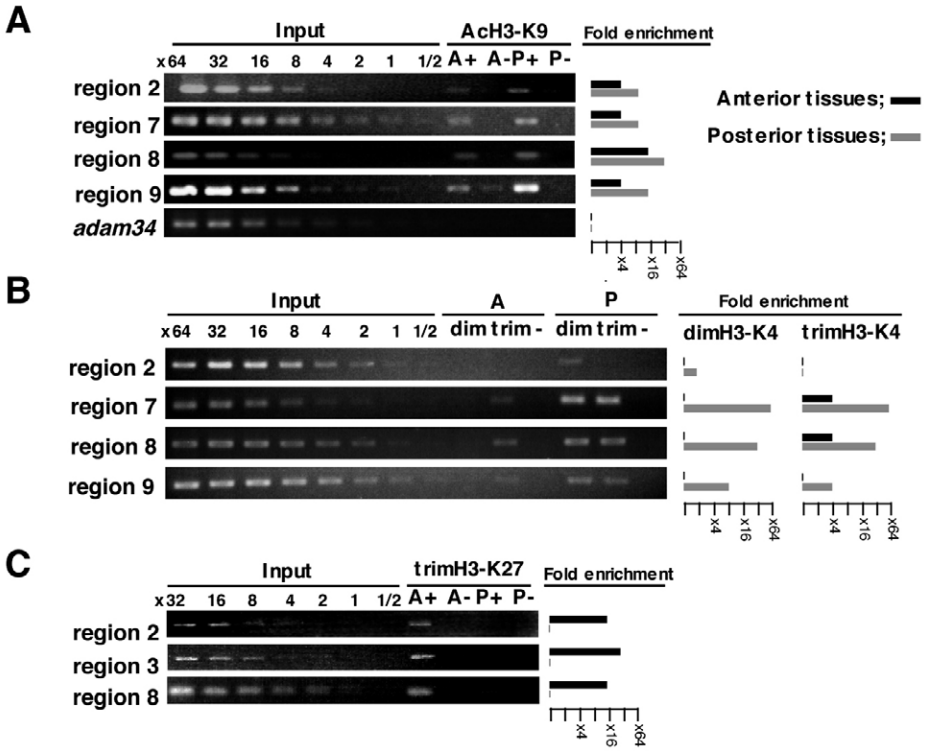

Fig. 2. Comparison of H3-K9 acetylation, H3-K4 methylation and H3-K27 trimethylation in *Hoxb8* genomic surrounding at 12.5 dpc between anterior and posterior tissues. (**A**) Comparative analysis of H3-K9 acetylation at regions 2, 7, 8 and 9. (Left) Whole-cell lysates (WCE) prepared from anterior and posterior parts of 12.5 dpc embryos were subjected to ChIP analyses by using anti-acetylated H3-K9. Amounts of immunoprecipitated genomic DNA (A+ and P+) by anti-acetylated H3-K9 subjected to PCR were equivalent to that of 'Input' DNA loaded in lane 1. Mock-immunoprecipitated DNA (A– and P–) derived from the same volume of the chromatin fraction as used for anti-acetylated H3-K9 immunoprecipitation were subjected to the PCR. (Right) Schematic comparison of H3-K9 acetylation between anterior and posterior tissues. The relative quantity of each genomic region in immunoprecipitated genomic DNA from anterior and posterior tissues was estimated by referring to 'Input' DNA isolated from the initial lysates and enrichment values against the initial lysate are represented by the black and gray bars, respectively. (**B**) Comparative analysis of di- and trimethylation of H3-K4 at the region 2, 7, 8 and 9. Representative results (left) and schematic summary (right) are shown. (**C**) Comparative analysis of trimethylation of H3-K27 at the region 2, 3 and 8. Representative results (left) and schematic summary (right) are shown.

(Yu et al., 1998). This suggests that this developmental stage might be the crucial period when PcG association and H3-K9 acetylation at *Hoxb8* play their role in modulating gene expression.

Prior to the ChIP analyses, we re-examined the expression of *Hoxb8* gene in the cranial and caudal tissues in quantitative manner by using real-time PCR (Fig. 3A). As reported previously by extensive in situ hybridization analyses, caudally restricted expression of *Hoxb8* was already established at 8.0 dpc and its relative quantity progressively increased until 12.5 dpc (Deschamps and Wijgerde, 1993). We carried out the kinetic analyses of the Rnf2 association, H3-K9 acetylation and H3-K27 trimethylation in early to later developmental stages across the *Hoxb8* promoter region (region 3 in Fig. 1F). In 8.0 dpc embryos, no Rnf2 association was seen at the six-somite stage. It was first seen, exclusively in cranial tissue, at the eight-somite stage (Fig. 3B). This was also the case at later stages up to 12.5 dpc (Fig. 3C-E). The relative quantity of Rnf2 association gradually increased and reached a maximal level at 10.5 dpc (Fig. 3E). H3-K9 acetylation was observed in the cranial region at the six-somite stage and in both cranial and caudal regions at the eight-somite stage. It was present at higher levels in the caudal region in 9.5 and 10.5 dpc embryos than in 8.0 dpc. H3-K27 trimethylation at region 3 continued to be seen in the cranial, but not in the caudal, region from 8.5 to 12.5 dpc. In summary, a differential association of Rnf2 with the *Hoxb8* promoter region, region 3, was established from 8.0 dpc onwards, and reached completion around 10.5 dpc (Fig. 3G) (Deschamps and Wijgerde, 1993). Relative amounts of acetylated H3-K9 in this region also increased up to 12.5 dpc. Likewise, differential trimethylation of H3-K27 was already established at 9.5 dpc and maintained to 12.5 dpc. These observations indicate that the Rnf2 association, H3-K9 acetylation and H3-K27 trimethylation may be involved to maintain the spatially restricted expression of the *Hoxb8*.

Evidence for the role of Rnf2 in transcriptional repression of Hox genes

Differential association of Rnf2 to *Hoxb8* genomic surrounding in tissues not expressing *Hoxb8* suggests its repressive role in *Hoxb8* transcription. This hypothesis is supported by our previous

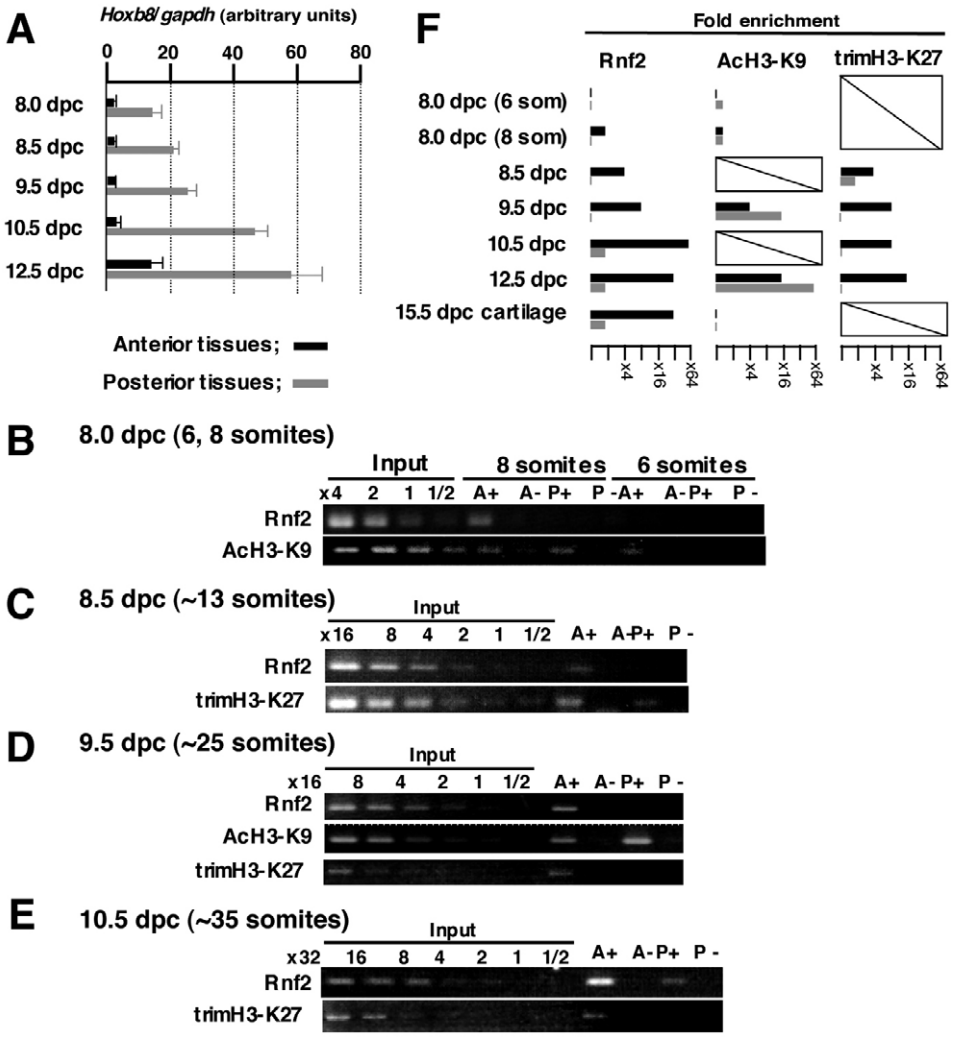

Fig. 3. Temporal changes in Rnf2 association, H3-K9 acetylation and H3-K27 trimethylation at the *Hoxb8* putative promotor region. (**A**) The expression of *Hoxb8* in the cranial and caudal tissues at various developmental stages, as quantified by using real-time PCR against the expression of *Gapdh*. Relative quantity was compared between anterior and posterior tissues. The *Hoxb8*/*Gapdh* ratio in the anterior tissue of 8.0 dpc embryo was arbitrarily 1. Embryos were bisected into the anterior and posterior tissues as described below. (**B**) Six- and eight-somite embryos were bisected at the level of the newly generated somite boundary and separated into anterior segmented (A) and posterior unsegmented (P) regions, and WCE prepared from respective tissues were subjected to ChIP analyses. (**C**) Embryos at the ~13-somite stage were dissected into three pieces at the boundary between somites 9 and 10, and at the newly generated somite boundary. WCE prepared from cranial region up to somite 9 (A) and posterior unsegmented region (P) were subjected to ChIP analyses. (**D**) Embryos at 9.5 dpc (about 25 somites) were bisected into anterior (A) and posterior (P) pieces at the level of somite 9/10 boundary and respective WCE were subjected to ChIP analyses. (**E**) Embryos at 10.5 dpc (~35 somites) were dissected at the level of the posterior end of the hindbrain and caudally to the forelimb bud after removing the viscera. For ChIP using anti-Rnf2, chromatin fractions prepared from the anterior (A) and posterior (P) tissues were used, whereas WCE were used for anti-acetylated H3-K9 and -trimethylated H3-K27 antibodies. (**F**) Schematic comparisons of Rnf2 association, H3-K9 acetylation and H3-K27 trimethylation at the region 3 between anterior and posterior tissues. The relative quantity of each genomic region in immunoprecipitated genomic DNA from anterior and posterior tissues was estimated by referring to those of 'Input' DNA isolated from the initial lysates and enrichment values against the 'Input' are represented by the black and gray bars, respectively. Stages left unexamined are indicated by boxes crossed with a diagonal line.

experiments that used an hypomorphic allele of *Rnf2*, in which the de-repression of several Hox genes was seen at 11.5 dpc (Suzuki et al., 2002). However, it was not determined whether Rnf2 association was functionally involved in the maintenance rather than early establishment of this repressed status. To address this question, we conditionally depleted functional *Rnf2* after the expression domain of *Hoxb8* was established. Because of early embryonic lethality of *Rnf2*-null mice, we generated a conditional allele designated as *Rnf2*^{fl} in which exon 2, containing the ATG initiation codon, was flanked with loxP sites (Voncken et al., 2003; de Napoles et al., 2004). Primary MEFs were derived from the cranial part of *Rnf2*$^{fl/fl}$ 9.5 dpc embryos in which *Hoxb8* expression was repressed. Subsequent deletion of *Rnf2* was achieved by infection of MEF cultures with adenovirus expressing the CRE recombinase (Ad-Cre) as described (de Napoles et al., 2004). Rnf2 depletion was evident in western analysis of infected cell culture (Fig. 4A) and took 2 days for completion. The analysis of *Hoxb8* expression continued for 4 days after Ad-Cre infection. Two independent experiments demonstrated more than a 16-fold increase of *Hoxb8* expression in infected MEFs compared with the uninfected control. Therefore Rnf2 association is essential for the maintenance of the transcriptional repression of *Hoxb8*.

After this, the repressive role of Rnf2 in undifferentiated embryonic stem (ES) cells was investigated because Hox repression was accompanied by both chromatin condensation of the Hox cluster and the location of the Hox genes within the chromosome territory, whereas decondensation and reorganization accompanied Hox gene expression both in ES cells and the developing neural tube (Chambeyron and Bickmore, 2004; Chambeyron et al., 2005).

Seven *Rnf2*$^{fl/fl}$ ES cells have been derived (de Napoles et al., 2004). *Rnf2*$^{-/-}$ ES cell derivatives of one of these lines, the male ES cell line, 13-3, were generated by CRE-mediated excision of exon 2 (Fig. 4B). Loss of functional Rnf2 resulted in de-repression of *Hoxa1*, *Hoxa7*, *Hoxb3*, *Hoxb8*, *Hoxb13*, *Hoxc9*, *Hoxd8* and *Hoxd10* but not of *Hoxc8* (Fig. 4C). To test if de-repression of Hox genes is a direct consequence of mutating Rnf2, complementation experiments were carried out, transfecting mutant ES cells with a construct expressing Myc-tagged Rnf2. As shown in Fig. 4B, transfected mutant ES cells expressed transgene-encoded Rnf2 at a level equivalent to half that of endogenous Rnf2. RT-PCR analysis revealed that the expression of *Hoxa1*, *Hoxb3*, *Hoxb8* and *Hoxd8* was repressed albeit not to the same degree as in the parental *Rnf2*$^{fl/fl}$ ES cells (Fig. 4C). These results confirm that Rnf2 association is required to mediate the transcriptional repression of Hox genes in ES cells.

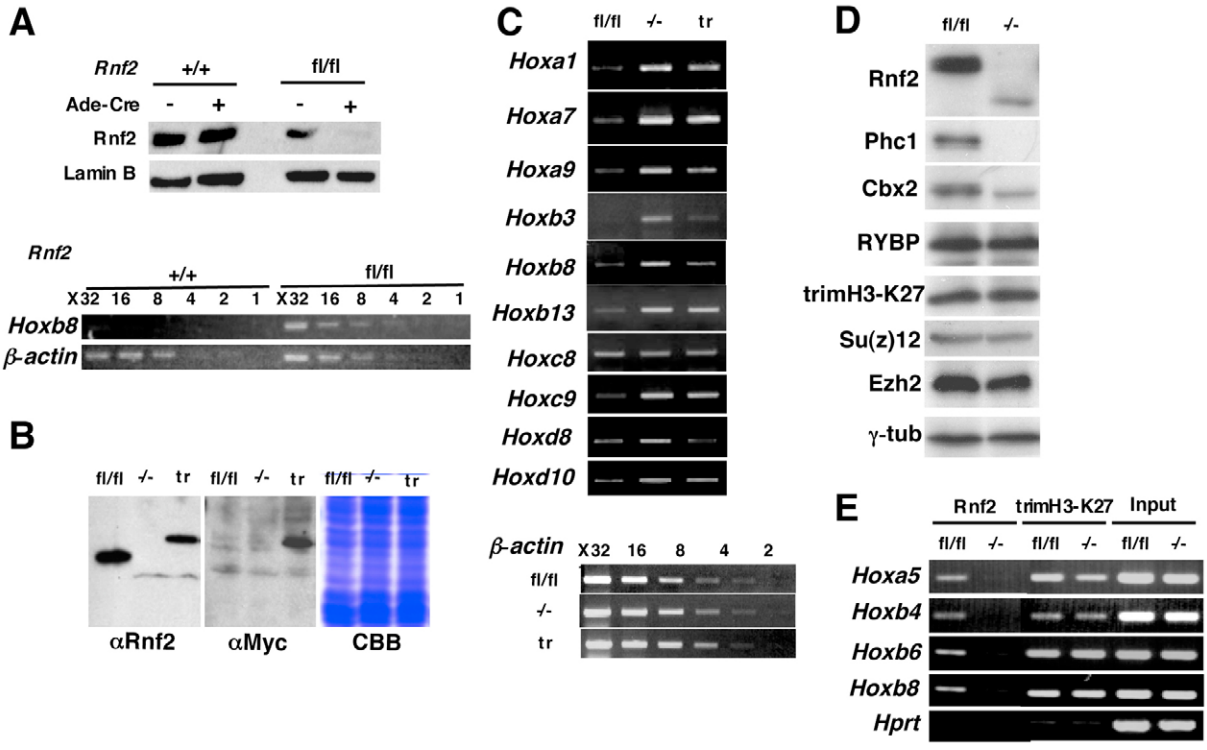

Fig. 4. De-repression of Hox genes in *Rnf2*$^{-/-}$ MEFs and ES cells. (**A**) Conditional depletion of Rnf2 lead to de-repression of *Hoxb8* in MEFs derived from the cranial part of *Rnf2*$^{fl/fl}$ 9.5 dpc embryos. (Top) Infection of Cre-expressing adenovirus vector to MEFs derived from *Rnf2*$^{fl/fl}$ embryos (fl/fl) depleted the Rnf2 gene products, whereas the wild-type (+/+) MEFs were unaffected. Lamin B was used as a control. (Bottom) The expression of Hoxb8 was induced by infection of Cre-expressing adenovirus vector in *Rnf2*$^{fl/fl}$ MEFs (fl/fl), but not in the wild type (+/+). (**B**) *Rnf2*$^{-/-}$ (–/–) ES cells were derived from *Rnf2*$^{fl/fl}$ (fl/fl) ES cells by transient overexpression of Cre-recombinase. Rnf2 was re-expressed by transfecting *Rnf2*$^{-/-}$ ES cells with a construct expressing Myc-tagged Rnf2 (tr). The expression of endogenous and transfected Rnf2 was examined by using anti-Rnf2 (left) and -Myc (middle) antibodies. CBB staining was used as a loading control (right). (**C**) The expression of Hox cluster genes in *Rnf2*$^{fl/fl}$ (fl/fl), *Rnf2*$^{-/-}$ (–/–) and Rnf2 transfected (tr) ES cells was compared by RT-PCR. The quantity of synthesized cDNA from respective cells was equalized by comparing the relative amounts of β-actin transcripts. (**D**) The expression of Phc1 and Cbx2 gene products was reduced in *Rnf2*$^{-/-}$ ES cells (–/–) in comparison with the wild type (fl/fl), whereas the expression of RYBP (another Rnf2-binding protein that is not found in hPRC-H complex or class 1 PcG proteins) was not altered. (**E**) Rnf2 association and H3-K27 trimethylation at Hox promoter regions were compared between *Rnf2*$^{fl/fl}$ and *Rnf2*$^{-/-}$ ES cells. For the 'Input', genomic DNA extracted from the original whole cell lysate equivalent to the 1/40 volume of that used for the ChIP analysis was subjected to the PCR. *Hprt* was used as a negative control.

Next, the method by which Rnf2 deficiency impacts on the functions of class 2 PcG complexes was investigated. As it has been suggested that Ring1 is an important component in the stabilization of the Polycomb core complex in Sf9 cells (Francis et al., 2001), the expression levels of other components of class 2 PcG complexes in *Rnf2*$^{-/-}$ ES cells was examined. The expression of both Phc1 and Cbx2 gene products was obviously reduced in *Rnf2*$^{-/-}$ ES cells (Fig. 4D; M.E. and H.K., unpublished). By contrast, the expression of RYBP, another Rnf2-binding protein, which is not found in hPRC-H complex, was not altered (Garcia et al., 1999) (Fig. 4D). As the transcription of *Phc1* and *Cbx2* was not altered in *Rnf2*$^{-/-}$ ES cells, Rnf2 loss specifically affects the expression of Phc1 and Cbx2. It is thus likely that Rnf2 impacts the Hox expression by regulating the stability of the class 2 PcG complexes.

The coincidence of Rnf2 association and H3-K27 trimethylation in transcriptionally repressed region further prompted us to ask whether de-repression of Hox genes in *Rnf2*$^{-/-}$ ES cells involves a change of H3-K27 trimethylation across the Hox genomic regions. The expression of Suz12 and Ezh2 were not significantly changed in *Rnf2*$^{-/-}$ ES cells (Fig. 4D). Concordant with this result, ChIP analyses revealed that local level of H3-K27 trimethylation at Hox promoter regions were almost unchanged (Fig. 4E). Therefore, Rnf2 deficiency affects Hox gene expressions without changing local H3-K27 trimethylation.

Functional involvement of trimethylated H3-K27 on Rnf2 association at Hox loci and on Hox gene expression

In *Drosophila*, trimethylation on H3-K27 has been shown to facilitate the recruitment of class 2 PcG complexes via direct interaction between trimethylated H3-K27 and the chromodomain of Pc (Cao et al., 2002; Czermin et al., 2002; Muller et al., 2002). Therefore, Hox gene expression and Rnf2 association at the *Hoxb* locus, in the absence of trimethylated H3-K27, was examined using *Suz12*$^{-/-}$ ES cells. We have independently generated a loss-of-function allele of *Suz12* and the homozygous mutants exhibited a phenotype almost identical to that reported by Pasini et al. (Pasini et al., 2004) (K.I. and H.K., unpublished). *Suz12*$^{-/-}$ ES cells were derived from crosses of heterozygous mutants. The absence of Suz12 reduced the levels of H3-K27 tri- and dimethylation to less than 10% of the wild type but did not significantly change H3-K9 methylation (Pasini et al., 2004). First, the association of class 1 PcG and H3-K27 trimethylation at the Hox promotor regions was investigated. Anti-Suz12, -Eed and -trimethylated H3-K27 antibodies specifically immunoprecipitated significant amounts of Hox promoter fragments from the wild-type ES cells (Fig. 5A). In *Suz12*$^{-/-}$ ES cells, no Hox DNA could be detected at all upon anti-Suz12 immunoprecipitation. The loss of Suz12 significantly reduced Eed association and H3-K27 trimethylation at Hox genes. Therefore, class 1 PcG complexes associate locally to Hox genes and mediate local H3-K27 trimethylation in undifferentiated ES cells. Second, the expression of *Hoxa1*, *Hoxa4*, *Hoxb1*, *Hoxb3*, *Hoxb4*, *Hoxb6*, *Hoxb8*, *Hoxb9* and *Hoxc6* was compared between wild-type and *Suz12*$^{-/-}$ ES cells by RT-PCR. *Suz12*$^{-/-}$ ES cells were shown to express more Hox gene transcripts than the wild type (Fig. 5B). Therefore, local H3-K27 trimethylation mediated by class 1 PcG complexes, or association of the complexes, are likely to be required in order to mediate repression of Hox genes. We went on to examine Rnf2 association in *Suz12*$^{-/-}$ ES cells. Rnf2 association to the Hox promoters was significantly reduced in *Suz12*$^{-/-}$ ES cells (Fig. 5A). Therefore H3-K27 trimethylation may be a prerequisite for the association of Rnf2 with Hox regulatory regions, as already demonstrated in *Drosophila*. The role of class 1 PcG complexes in the recruitment of the class 2 complexes via protein-protein interactions is not necessarily excluded.

The positive role of PcG complexes on transcription is coupled to increased H3-K9 acetylation

Results from this study also show that PcG gene products associate to *Hoxb8* genomic regions in the transcriptionally active caudal embryonic tissues. This is in line with the recently uncovered positive function of class 2 PcG complexes (de Graaff et al., 2003). Null mutations in the *Rnf110* and *Phc1* loci have been shown to decrease the transcription level of endogenous *Hoxb1*, and to severely impair the transcription from Hox/*lacZ* reporters and knock-in loci (de Graaff et al., 2003). In addition, a positive action of PcG complexes explains the drop in gene expression levels within the *Hoxb8* expression domains known to occur around 9.5 dpc in *Bmi1/Rnf110* and *Phc1/Phc2* double mutants (Akasaka et al., 2001; de Graaff et al., 2003; Isono et al., 2005b). As the level of histone H3 acetylation correlates with Hox gene expression in *Mll* mutants and controls, and Mll and Bmi1 proteins display discrete subnuclear colocalization, we investigated whether the drop in *Hoxb8* expression level in *Rnf110/Bmi1* and *Phc1/Phc2* double mutants involved a change in H3-K9 acetylation (Hanson et al., 1999; Milne et al., 2002; de Graaff et al., 2003). The degree of H3-K9 acetylation in the caudal region of *Rnf110*$^{-/-}$*Bmi1*$^{-/-}$ embryos was much lower

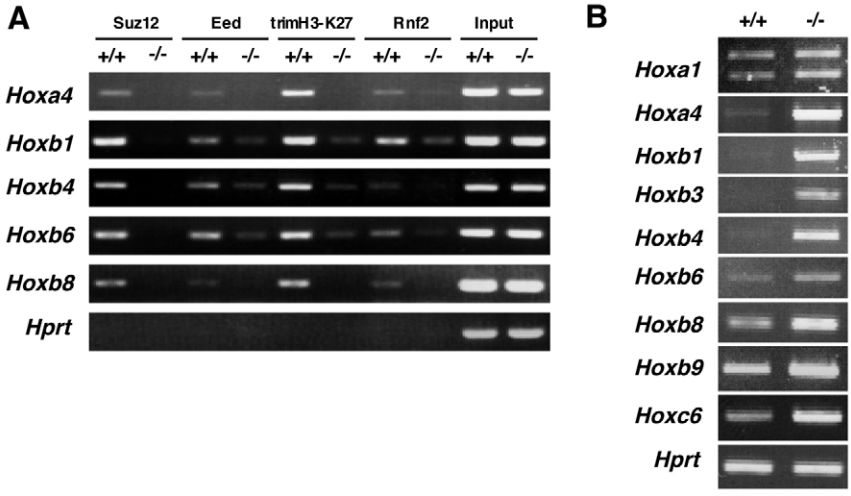

Fig. 5. De-repression of Hox genes in *Suz12*$^{-/-}$ ES cells correlates with reduction of Rnf2 association to Hox genomic regions. (**A**) The association of Suz12, Eed, Rnf2 and H3-K27 trimethylation at the Hox promoter regions in the wild-type and *suz12*$^{-/-}$ ES cells. Whole-cell lysates prepared from approximately the same number of wild type (+/+) and *suz12*$^{-/-}$ (–/–) ES cells were subjected to ChIP analyses using anti-Suz12, -Eed, -trimethylated H3-K27 and -Rnf2 antibodies. For the 'Input', genomic DNA extracted from the original whole cell lysate equivalent to the 1/40 volume of that used for the ChIP analysis was subjected to the PCR. *Hprt* was used as a control. (**B**) The expression of Hox cluster genes in the wild type (+/+) and *suz12*$^{-/-}$ (–/–) ES cells was compared by RT-PCR.

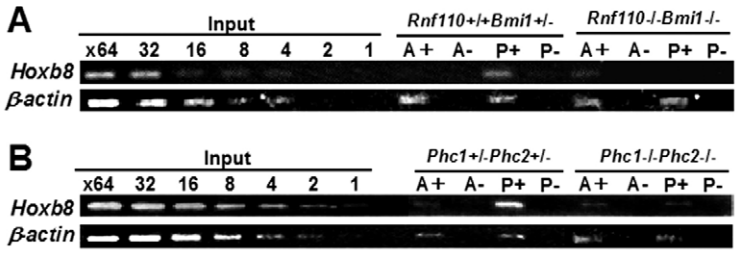

Fig. 6. Decreased H3-K9 acetylation at the first exonic region of *Hoxb8* in the posterior tissues of *Rnf110*$^{-/-}$*Bmi1*$^{-/-}$ and *Phc1*$^{-/-}$*Phc2*$^{-/-}$ embryos at 9.5 dpc. (**A**) Degree of H3-K9 acetylation in the anterior (A) and posterior (P) regions were compared in *Rnf110*$^{+/-}$*Bmi1*$^{+/-}$ and *Rnf110*$^{-/-}$*Bmi1*$^{-/-}$ embryos. The β-actin promoter was used as a positive control. (**B**) Degree of H3-K9 acetylation in the anterior (A) and posterior (P) regions were compared in *Phc1*$^{-/-}$*Phc2*$^{+/-}$, *Phc1*$^{+/-}$*Phc2*$^{-/-}$ and *Phc1*$^{-/-}$*Phc2*$^{-/-}$ embryos. The β-actin promoter was used as a positive control. In this study, the negative control ChIPs (A– and P–) were performed with rabbit IgG.

than in *Rnf110*$^{+/+}$*Bmi1*$^{+/-}$, whereas the H3-K9 acetylation at the β-actin promoter was almost equivalent (Fig. 6A). Similarly, H3-K9 acetylation level in the caudal part of *Phc1*$^{-/-}$*Phc2*$^{-/-}$ was equivalent to the cranial part whereas craniocaudally graded acetylation was seen in *Phc1*$^{+/-}$*Phc2*$^{+/-}$ embryos (Fig. 6B). Therefore association of class 2 PcG gene products to *Hox*b8 is required for the maintenance of H3-K9 acetylation in transcriptionally active regions.

DISCUSSION

The main outcome of this study was to show that binding of a specific, Rnf2-containing form of the class 2 PcG complex, as well as H3-K27 trimethylation marking inactive chromatin, correlates with the maintenance of transcriptional silencing of a Hox gene in developing embryos. Moreover, the results demonstrated that genetic impairment of both PcG binding, and H3-K27 trimethylation leads to Hox gene derepression, and that H3-K27 trimethylation is required for PcG binding. In addition, we showed that the establishment of differential PcG binding and histone marks in expressing and non-expressing embryonic tissues occur in the same developmental time window as when Hox genes are deregulated in *PcG* mutants.

Rnf2 association to known regulatory elements of the *Hoxb8* gene is seen predominantly in transcriptionally silent anterior embryonic tissues, whereas the binding of other PcG class 2 members, Phc1 and Cbx2, is observed at all AP levels, irrespective of transcriptional status. This implies that different forms of class 2 PcG complexes bind to the Hoxb genomic region in embryonic domains where the gene is transcriptionally active and repressed. This is reminiscent of previous findings in the *Engrailed/Inv/GeneVI* complex in *Drosophila* SL-2 cells, where the Pc protein is exclusively associated with transcriptionally silent genes, while Ph and Psc are present irrespective of the transcriptional status (Strutt and Paro, 1997). Therefore the complete, 'perfect' form of the class 2 PcG core complex may mediate transcriptional repression more efficiently than form(s) lacking the Rnf2 component. If this is the case, incorporation of the Rnf2 component into the complex might be a limiting process to mediate transcriptional repression and regulate its stability (Francis et al., 2001). It is also possible that the role of Rnf2 is mediated through its E3 ubiquitin ligase activity directed to histone H2A (Wang et al., 2004a; de Napoles et al., 2004).

Transcriptional repression of Hox genes in the developing embryo has been shown to correlate with the association of Rnf2-containing class 2 PcG complexes and H3-K27 trimethylation. De-repression of Hox genes in *Rnf2* and *Suz12* mutant cells reveal the requirement of both Rnf2 association and H3-K27 trimethylation in the mediation of this transcriptional repression. As Rnf2 association to Hox genes is reduced in *Suz12* mutant ES cells and *Rnf2* mutation alters Hox expression without changing local levels of H3-K27 trimethylation, H3-K27 trimethylation mediated by class 1 PcG complexes at Hox genes may facilitate subsequent binding of Rnf2-containing PcG complexes. Recruitment of Rnf2-containing PcG complexes may in turn prevent the access of nucleosome remodeling factors, such as SWI/SNF complex, leading to the formation of a repressed chromatin status (Shao et al., 1999; Levine et al., 2002). Therefore, molecular circuitry underlying PcG silencing of Hox genes seems to have been evolutionarily conserved between *Drosophila* and mammals. It is also notable that Cbx2, a homologue of *Drosophila* Pc, binds to *Hoxb8* in transcriptionally active embryonic tissues, despite the lack of histone H3 trimethylated at K27. This is consistent with previous biochemical data that have shown the association of purified or reconstituted PcG complexes with the nucleosomal templates lacking histone tails (Shao et al., 1999). The implication of these findings is that there are at least two different means by which class 2 PcG complexes bind to the chromatin, and that the association, which involves trimethylated H3-K27, mediates the repression at the Hox genes in vivo (Cao et al., 2002; Czermin et al., 2002; Muller et al., 2002).

The maintenance of regionally restricted expression of Hox genes is likely to involve H3-K9 acetylation and H3-K4 methylation (Milne et al., 2002; Rastegar et al., 2004). We have shown that these modifications of the histone tail increases craniocaudally along the axis. Although the transcriptionally active posterior tissues of 9.5 dpc and older embryos are more heavily acetylated at H3-K9 than the anterior, non-Hox expressing tissues, some acetylation of H3-K9 at *Hoxb8* is seen in anterior regions where *Hoxb8* expression is repressed at early and later developmental stages. De-repression of *Hoxb8* expression upon depletion of Rnf2 in MEFs derived from the cranial part of 9.5 dpc embryos suggests the involvement of Rnf2-containing class 2 PcG complexes to mediate this transcriptional repression. Therefore, our data suggest that the associations of Rnf2-containing PcG complexes and acetylated H3-K9 may counteract each other and cooperate to maintain the anterior boundaries of *Hoxb8* expression at mid-gestational stages and later. This is consistent with the antagonistic properties of *Mll* and *Bmi1* mutations (Hanson et al., 1999). Moreover, the establishment of the differential binding of the Rnf2 and H3-K9 acetylation at *Hoxb8* during embryogenesis temporally coincides with de-repression of that Hox gene in *Bmi1/Rnf110* and *Phc1/Phc2* double homozygotes, and loss of its transcription in *Mll* homozygotes (Akasaka et al., 2001; Yu et al., 1998; Isono et al., 2005b). Intriguingly, class 2 PcG complexes, which lack the Rnf2 component, are also involved in the maintenance of H3-K9 acetylation in embryonic tissues where Hox genes are expressed. This is consistent with predominant subnuclear localization of several PcG proteins in the perichromatin compartment where most pre-mRNA synthesis takes place (Cmarco et al., 2003). The molecular mechanisms underlying this positive action remain unaddressed.

In conclusion, class 2 PcG gene products play distinct roles in embryonic territories, which are silent or active for *Hoxb8* transcription, by forming complexes of different composition. Interaction between class 1 and class 2 PcG complexes mediated by

trimethylated H3-K27 play decisive roles in Hox gene repression outside their expression domains, as seen in *Drosophila*. In addition, within the Hox expression domain, class 2 PcG complexes are involved in maintaining a transcriptionally active status, independent of H3-K27 trimethylation.

Supplementary material

Supplementary material for this article is available at http://dev.biologists.org/cgi/content/full/133/12/2371/DC1

References

Agalioti, T., Chen, G. and Thanos, D. (2002). Deciphering the transcriptional histone acetylation code for a human gene. *Cell* **111**, 381-392.

Akasaka, T., Kanno, M., Mieza, M. A., Balling, R., Taniguchi, M. and Koseki, H. (1996). A role for mel-18, a Polycomb group-related vertebrate gene, during the anteroposterior specification of the axial skeleton. *Development* **122**, 1513-1522.

Akasaka, T., van Lohuizen, M., van der Lugt, N., Mizutani-Koseki, Y., Kanno, M., Taniguchi, M., Vidal, M., Alkema, M., Berns, A. and Koseki, H. (2001). Mice doubly deficient for the Polycomb Group genes Mel18 and Bmi1 reveal synergy and requirement for maintenance but not initiation of Hox gene expression. *Development* **128**, 1587-1597.

Atsuta, T., Fujimura, S., Moriya, H., Vidal, M., Akasaka, T. and Koseki, H. (2001). Production of monoclonal antibodies against mammalian Ring1B proteins. *Hybridoma* **20**, 43-46.

Brachvogel, B., Reichenberg, D., Beyer, S., Jehn, B., von der Mark, K. and Bielke, W. (2002). Molecular cloning and expression analysis of a novel member of the Disintegrin and Metalloprotease-Domain (ADAM) family. *Gene* **288**, 203-210.

Cao, R., Wang, L., Wang, H., Xia, L., Erdjument-Bromage, H., Tempst, P., Jones, R. S. and Zhang, Y. (2002). Role of histone H3 lysine 27 methylation in Polycomb-group silencing. *Science* **298**, 1039-1043.

Cavalli, G. and Paro, R. (1998). The Drosophila Fab-7 chromosomal element conveys epigenetic inheritance during mitosis and meiosis. *Cell* **93**, 505-518.

Chambeyron, S. and Bickmore, W. A. (2004). Chromatin decondensation and nuclear reorganization of the HoxB locus upon induction of transcription. *Genes Dev.* **18**, 1119-1130.

Chambeyron, S., Da Silva, N. R., Lawson, K. A. and Bickmore, W. A. (2005). Nuclear reorganization of the HoxB complex during mouse embryonic development. *Development* **132**, 2215-2223.

Charité, J., de Graaff, W., Vogels, R., Meijlink, F. and Deschamps, J. (1995). Regulation of the Hoxb-8 gene: synergism between multimerized cis-acting elements increases responsiveness to positional information. *Dev. Biol.* **171**, 294-305.

Cmarko, D., Verschure, P. J., Otte, A. P., van Driel, R. and Fakan, S. (2003). Polycomb group gene silencing proteins are concentrated in the perichromatin compartment of the mammalian nucleus. *J. Cell Sci.* **116**, 335-343.

Czermin, B., Melfi, R., McCabe, D., Seitz, V., Imhof, A. and Pirrotta, V. (2002). Drosophila enhancer of Zeste/ESC complexes have a histone H3 methyltransferase activity that marks chromosomal Polycomb sites. *Cell* **111**, 185-196.

de Graaff, W., Tomotsune, D., Oosterveen, T., Takihara, Y., Koseki, H. and Deschamps, J. (2003). Randomly inserted and targeted Hox/reporter fusions transcriptionally silenced in Polycomb mutants. *Proc. Natl. Acad. Sci. USA* **100**, 13362-13367.

de Napoles, M., Mermoud, J. E., Wakao, R., Tang, Y. A., Endoh, M., Appanah, R., Nesterova, T. B., Silva, J., Otte, A. P., Vidal, M. et al. (2004). Polycomb group proteins Ring1A/B link ubiquitylation of histone H2A to heritable gene silencing and X inactivation. *Dev. Cell* **7**, 663-676.

Deschamps, J. and Wijgerde, M. (1993). Two phases in the establishment of *Hox* expression domains. *Dev. Biol.* **152**, 473-480.

Fischle, W., Wang, Y. and Allis, C. D. (2003). Binary switches and modification cassettes in histone biology and beyond. *Nature* **425**, 475-479.

Francis, N. J., Saurin, A. J., Shao, Z. and Kingston, R. E. (2001). Reconstitution of a functional core polycomb repressive complex. *Mol. Cell* **8**, 545-556.

Garcia, E., Marcos-Gutierrez, C., del Mar Lorente, M., Moreno, J. C. and Vidal, M. (1999). RYBP, a new repressor protein that interacts with components of the mammalian Polycomb complex, and with the transcription factor YY1. *EMBO J.* **18**, 3404-3418.

Hamer, K. M., Sewalt, R. G., den Blaauwen, J. L., Hendrix, T., Satijn, D. P. and Otte, A. P. (2002). A panel of monoclonal antibodies against human polycomb group proteins. *Hybrid. Hybridomics* **21**, 245-252.

Hanson, R. D., Hess, J. L., Yu, B. D., Ernst, P., van Lohuizen, M., Berns, A., van der Lugt, N. M., Shashikant, C. S., Ruddle, F. H., Seto, M. et al. (1999). Mammalian Trithorax and polycomb-group homologues are antagonistic regulators of homeotic development. *Proc. Natl. Acad. Sci. USA* **96**, 14372-14377.

Isono, K., Mizutani-Koseki, Y., Komori, T., Schmidt-Zachmann, M. S. and Koseki, H. (2005a). Mammalian Polycomb-mediated repression of *Hox* genes requires the essential spliceosomal protein Sf3b1. *Genes Dev.* **19**, 536-541.

Isono, K., Fujimura, Y., Shinga, J., Yamaki, M., O-Wang, J., Takihara, Y., Murahashi, Y., Takada, Y., Mizutani-Koseki, Y. and Koseki, H. (2005b). Mammalian polyhomeotic homologues Phc2 and Phc1 act in synergy to mediate Polycomb-repression of *Hox* genes. *Mol. Cell. Biol.* **25**, 6694-6706.

Kanegae, Y., Lee, G., Sato, Y., Tanaka, M., Nakai, M., Sakaki, T., Sugano, S. and Saito, I. (1995). Efficient gene activation in mammalian cells by using recombinant adenovirus expressing site-specific Cre recombinase. *Nucleic Acids Res.* **23**, 3816-3821.

Kennison, J. A. and Tamkun, J. W. (1988). Dosage-dependent modifiers of Polycomb and antennapedia mutations in Drosophila. *Proc. Natl. Acad. Sci. USA* **85**, 8136-8140.

King, I. F., Francis, N. J. and Kingston, R. E. (2002). Native and recombinant Polycomb group complexes establish a selective block to template accessibility to repress transcription in vitro. *Mol. Cell. Biol.* **22**, 7919-7928.

Lachner, M., O'Sullivan, R. J. and Jenuwein, T. (2003). An epigenetic road map for histone lysine methylation. *J. Cell Sci.* **116**, 2117-2124.

Levine, S. S., Weiss, A., Erdjument-Bromage, H., Shao, Z., Tempst, P. and Kingston, R. E. (2002). The core of the Polycomb repressive complex is compositionally and functionally conserved in flies and humans. *Mol. Cell. Biol.* **22**, 6070-6078.

Milne, T. A., Briggs, S. D., Brock, H. W., Martin, M. E., Gibbs, D., Allis, C. D. and Hess, J. L. (2002). MLL targets SET domain methyltransferase activity to Hox gene promoters. *Mol. Cell* **10**, 1107-1117.

Miyagishima, H., Isono, K., Fujimura, Y., Iyo, M., Takihara, Y., Masumoto, H., Vidal, M. and Koseki, H. (2003). Dissociation of mammalian Polycomb-group proteins, Ring1B and Rae28/Ph1, from the chromatin correlates with configuration changes of the chromatin in mitotic and meiotic prophase. *Histochem. Cell Biol.* **120**, 111-119.

Muller, J., Hart, C. M., Francis, N. J., Vargas, M. L., Sengupta, A., Wild, B., Miller, E. L., O'Connor, M. B., Kingston, R. E. and Simon, J. A. (2002). Histone methyltransferase activity of a Drosophila Polycomb group repressor complex. *Cell* **111**, 197-208.

Nakamura, T., Mori, T., Tada, S., Krajewski, W., Rozovskaia, T., Wassell, R., Dubois, G., Mazo, A., Croce, C. M. and Canaani, E. (2002). ALL-1 is a histone methyltransferase that assembles a supercomplex of proteins involved in transcriptional regulation. *Mol. Cell* **10**, 1119-1128.

Oosterveen, T., Niederreither, K., Dolle, P., Chambon, P., Meijlink, F. and Deschamps, J. (2003). Retinoids regulate the anterior expression boundaries of 5′ Hoxb genes in posterior hindbrain. *EMBO J.* **22**, 262-269.

Orlando, V., Strutt, H. and Paro, R. (1997). Analysis of chromatin structure by in vivo formaldehyde cross-linking. *Methods* **11**, 205-214.

Paro, R. (1995). Propagating memory of transcriptional states. *Trends Genet.* **11**, 295-297.

Pasini, D., Bracken, A. P., Jensen, M. R., Denchi, E. L. and Helin, K. (2004). Suz12 is essential for mouse development and for EZH2 histone methyltransferase activity. *EMBO J.* **23**, 4061-4071.

Peters, A. H., Kubicek, S., Mechtler, K., O'Sullivan, R. J., Derijck, A. A., Perez-Burgos, L., Kohlmaier, A., Opravil, S., Tachibana, M., Shinkai, Y. et al. (2003). Dec Partitioning and plasticity of repressive histone methylation states in mammalian chromatin. *Mol. Cell* **12**, 1577-1589.

Pirrotta, V. (1997). PcG complexes and chromatin silencing. *Curr. Opin. Genet. Dev.* **7**, 249-258.

Rastegar, M., Kobrossy, L., Kovacs, E. N., Rambaldi, I. and Featherstone, M. (2004). Sequential histone modifications at Hoxd4 regulatory regions distinguish anterior from posterior embryonic compartments. *Mol. Cell. Biol.* **24**, 8090-8103.

Schoorlemmer, J., Marcos-Gutierrez, C., Were, F., Martinez, R., Garcia, E., Satijn, D. P., Otte, A. P. and Vidal, M. (1997). Ring1A is a transcriptional repressor that interacts with the Polycomb-M33 protein and is expressed at rhombomere boundaries in the mouse hindbrain. *EMBO J.* **16**, 5930-5942.

Shao, Z., Raible, F., Mollaaghababa, R., Guyon, J. R., Wu, C. T., Bender, W. and Kingston, R. E. (1999). Stabilization of chromatin structure by PRC1, a Polycomb complex. *Cell* **98**, 37-46.

Shumacher, A., Faust, C. and Magnuson, T. (1996). Positional cloning of a global regulator of anterior-posterior patterning in mice. *Nature* **383**, 250-253.

Strutt, H. and Paro, R. (1997). The polycomb group protein complex of Drosophila melanogaster has different compositions at different target genes. *Mol. Cell. Biol.* **17**, 6773-6783.

Suzuki, M., Mizutani-Koseki, Y., Fujimura, Y., Miyagishima, H., Kaneko, T., Takada, Y., Akasaka, T., Tanzawa, H., Takihara, Y., Nakano, M. et al. (2002). Involvement of the Polycomb-group gene Ring1B in the specification of the anterior-posterior axis in mice. *Development* **129**, 4171-4183.

Takihara, Y., Tomotsune, D., Shirai, M., Katoh-Fukui, Y., Nishii, K., Motaleb, M. A., Nomura, M., Tsuchiya, R., Fujita, Y., Shibata, Y. et al. (1997). Targeted disruption of the mouse homologue of the Drosophila polyhomeotic gene leads to altered anteroposterior patterning and neural crest defects. *Development* **124**, 3673-3682.

Tamkun, J. W., Deuring, R., Scott, M. P., Kissinger, M., Pattatucci, A. M.,

Kaufman, T. C. and Kennison, J. A. (1992). brahma: a regulator of Drosophila homeotic genes structurally related to the yeast transcriptional activator SNF2/SWI2. *Cell* **68**, 561-572.
van der Lugt, N. M., Alkema, M., Berns, A. and Deschamps, J. (1996). The Polycomb-group homolog Bmi-1 is a regulator of murine Hox gene expression. *Mech. Dev.* **58**, 153-164.
van der Vlag, J. and Otte, A. P. (1999). Transcriptional repression mediated by the human polycomb-group protein EED involves histone deacetylation. *Nat. Genet.* **23**, 474-478.
Vogels, R., Charite, J., de Graaff, W. and Deschamps, J. (1993). Proximal cis-acting elements cooperate to set Hoxb-7 (Hox-2.3) expression boundaries in transgenic mice. *Development* **118**, 71-82.
Voncken, J. W., Roelen, B. A., Roefs, M., de Vries, S., Verhoeven, E., Marino, S., Deschamps, J. and van Lohuizen, M. (2003). Rnf2 (Ring1b) deficiency causes gastrulation arrest and cell cycle inhibition. *Proc. Natl. Acad. Sci. USA* **100**, 2468-2473.
Wang, H., Wang, L., Erdjument-Bromage, H., Vidal, M., Tempst, P., Jones, R. S. and Zhang, Y. (2004a). Role of histone H2A ubiquitination in Polycomb silencing. *Nature* **431**, 873-878.
Wang, L., Brown, J. L., Cao, R., Zhang, Y., Kassis, J. A. and Jones, R. S. (2004b). Hierarchical recruitment of polycomb group silencing complexes. *Mol. Cell* **14**, 637-646.
Yu, B. D., Hanson, R. D., Hess, J. L., Horning, S. E. and Korsmeyer, S. J. (1998). MLL, a mammalian trithorax-group gene, functions as a transcriptional maintenance factor in morphogenesis. *Proc. Natl. Acad. Sci. USA* **95**, 10632-10636.